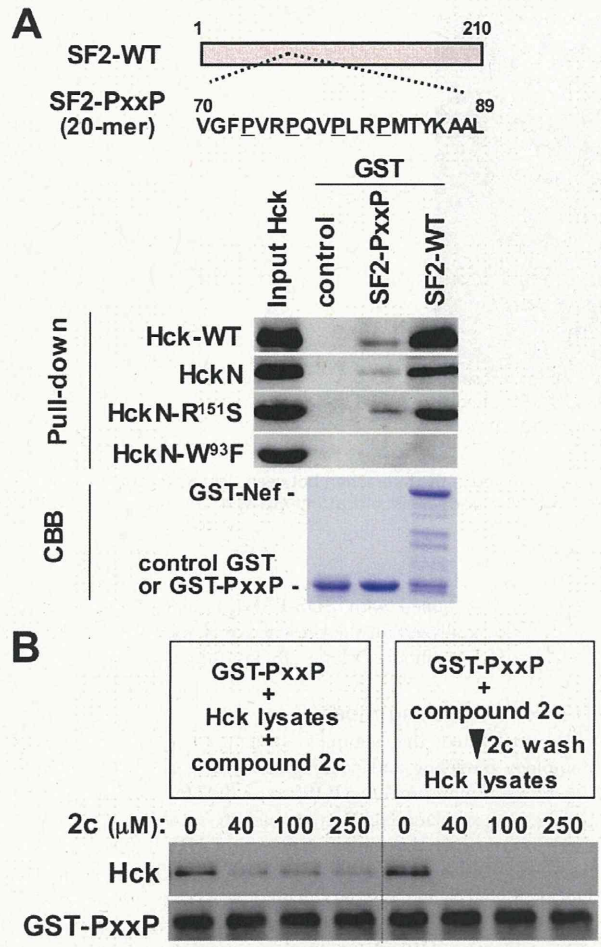

Figure 8. The effect of 2c on the binding between Nef PxxP motif-containing peptides and Hck. (A) The Nef peptide fused to GST is shown schematically. The 20 amino acid peptide derived from the PxxP motif of SF2 Nef was used (the proline residues are underlined). The resins to which the control GST, GST-SF2 Nef-PxxP peptides (SF2-PxxP), or GST-intact SF2 Nef (SF2-WT) fusion proteins were bound were incubated with the lysates of 293 cells expressing the indicated Hck protein. The amount of Hck bound to each resin was determined by Western blotting (Pull-down). To verify the equal expression of these Hck proteins in the 293 cells, equal amounts of each cell lysate were analyzed (Input Hck). Moreover, the amounts of the GST and GST-Nef fusion proteins bound to the resins were verified by eluting from the resins followed by SDS-PAGE/Coomassie brilliant blue (CBB) staining. (B) Two different competitive pull-down assays were performed. In the experiment shown in the left panel, the resins to which the GST-SF2 Nef-PxxP peptides were bound were incubated with the lysates of 293 cells expressing the wild-type Hck and the indicated concentration of 2c. In the experiment shown in the right panel, the resins to which the GST-SF2 Nef-PxxP peptides were bound were incubated with the indicated concentrations of 2c for 4 h and then washed to remove unbound 2c. Then, the resins were incubated with the lysates of 293 cells expressing the wild-type Hck. The amount of Hck bound to the resins was determined by Western blotting (upper blots). The GST-Nef blot was used as a loading control (lower blots). Data shown are representative of two independent experiments with similar results.
doi:10.1371/journal.pone.0027696.g008

care), the Immunostar LD Western blotting detection reagent (Wako, Osaka, Japan), and an image analyzer (ImageQuant LAS 4000; GE Healthcare).

Infectivity assay

TZM-bl cells (NIH AIDS Research & Reference Program) were maintained in DME medium supplemented with 10% FCS and used as viral target cells. TZM-bl cells were seeded onto 96-well tissue culture plates at a density of 6×10^3 cells/well and challenged with serially diluted viruses normalized for the concentration of p24 Gag protein. The supernatant of the proviral plasmid-transfected 293 cells was used as a viral stock and diluted with DME medium containing 10% FCS and 20 μg/ml DEAE-dextran (MP Biomedicals, Solon, OH). The diluted viruses were then added to the target cells (150 μl/well) overnight, and the culture medium was replaced with fresh DME medium containing 10% FCS and incubated for 48 h. In a selected experiment (see Fig. 2A), 2c was added to TZM-bl cells together with the diluted viruses. Viral infectivity was assessed by measuring the HIV-1 Tat-mediated induction of β-galactosidase activity in the target cells using a β-Galactosidase Enzyme Assay System (Promega). The absorbance of the wells was measured at 420 nm using a Multiskan microplate reader (Thermo Electron).

Replication assay

The replication assay with macrophages was performed essentially as described previously [46]. Heparinized venous blood was collected from healthy donors, after informed consent was obtained in accordance with the Declaration of Helsinki. The approval for this study was obtained from the Kumamoto University Medical Ethical Committee. Mononuclear cells obtained using LSM reagent (MP Biomedicals) were suspended into RPMI1640 medium-1% FCS at 1×10^6 cells/ml and seeded into 24-well plates. Monocytes were enriched by adherence to plates for 1 h at 37°C, and non-adherent cells were removed by extensive washing with PBS. Then, the adherent monocytes were differentiated into macrophages by culturing with RPMI1640-10% FCS containing 100 ng/ml rhM-CSF (a gift from Morinaga Milk Industry, Kanagawa, Japan). After 3 days, the cultures were replaced with fresh complete media and incubated for another 3 days. The purity of the day 6-macrophages prepared by this method was routinely more than 95% when assessed by the expression of CD14 (data not shown). Then, macrophages were incubated with 250 μl of the 293 cell supernatants containing JRFL HIV-1 viruses for 2 h at 37°C. Either 2c or DMSO was added to the incubation together with the diluted viruses. AZT (NIH AIDS Research & Reference Program) was used as a positive control. The cells were washed twice with PBS to remove unbound viruses and cultured with RPMI1640-10% FCS containing rhM-CSF in the presence or absence of 2c or AZT. One-half of the culture media was replaced with the complete media every 3 days. The culture supernatants collected at day 6, 9 and 12 were analyzed for the concentration of p24 Gag proteins by ELISA to monitor viral replication.

Jurkat cells were also used in this study. The cell pellet (1×10^6 cells) were incubated with 500 μl of the 293 cell supernatants containing NL43 viruses for 2 h at 37°C. Either 2c or DMSO was added to the incubation together with the diluted viruses. AZT was used as a positive control. The cells were washed twice with PBS, resuspended into 1 ml of RPMI1640-10% FCS, and cultured for 3 days in the presence or absence of 2c or AZT. Then, the culture were diluted (1/5) with RPMI1640-10% FCS, and cultured for another 2 days in the presence or absence of 2c or AZT. The concentration of p24 in the culture supernatants of day 5, 7 and 9 was analyzed as above.

GST pull-down assay

The control GST and GST-Nef fusion proteins cloned in the pGEX-6P-1 vector were expressed in *E. coli* BL21 cells

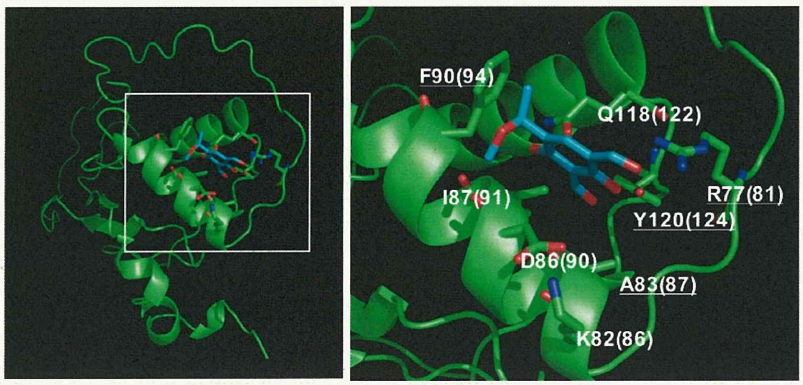

Figure 9. The 2c-Nef docking model. The amino acids that are predicted to be involved in the interaction between Nef and 2c are indicated. The positions of these amino acids in the NL43 strain and SF2 strain are shown. The amino acids predicted to interact with the Hck SH3 domain are underlined [38].
doi:10.1371/journal.pone.0027696.g009

(GE Healthcare). The cells were grown in LB medium containing 50 μg/ml ampicillin, before being induced with 1 μM IPTG (Sigma). The expression-induced cells were harvested and lysed with BugBuster Protein Extraction Reagent containing 1 U/ml rLysozyme and 25 U/ml Benzonase Nuclease (all from Novagen). The cleared lysates were then incubated with GST-Bind Resin (Novagen). After extensive washing with GST Bind/Wash Buffer (Novagen), the resin was incubated with the total cell lysate of the 293 cells transfected with the expression plasmid for Hck for 12 h. In the competitive pull-down assay, we employed the following 3 protocols: (1) the concurrent addition of 2c and Hck-containing lysates to the GST-Nef-bound resin, (2) the addition of Hck-containing lysates for 3 h followed by the addition of 2c, (3) the addition of 2c at the indicated concentrations for 4 h followed by the addition of the Hck-containing lysates. The incubation of the above mixtures was carried out at 4°C in Nonidet P-40 lysis buffer (1% Nonidet P-40, 50 mM Tris, and 150 mM NaCl) containing protease inhibitors (1 mM EDTA, 1 μM PMSF, 1 μg/ml aprotinin, 1 μg/ml leupeptin, and 1 μg/ml pepstatin). After extensive re-washing with complete Nonidet P-40 lysis buffer, the resin was boiled with SDS-PAGE sample buffer, and the eluates were analyzed for the presence of Hck by Western blotting with anti-Hck antibodies (clone 18; Transduction Laboratories).

The 2c-Nef docking model

We predicted the complex structures of Nef and 2c by homology modeling and docking simulation using the Molecular Operating Environment (MOE) ver. 2007.09. (Chemical Computing Group, Canada). First, homology modeling [47–49] was used to construct the model structure of HIV-1 Nef SF2 strain using its NMR structure (PDB code: 2NEF) [50] as a template. During the modeling, energy calculations were performed with the AMBER ff99 force field [51] and the GB/VI implicit solvent energy function [52]. Next, docking simulation of 2c with the homology model of Nef was achieved with the ASEDock module [53]. The initial structure of 2c was generated with the Molecular Builder module. Then, we searched for the binding site of 2c with the Site-Finder module. During the simulation, the energy calculations were performed with the MMFF94x force field [54,55] and the GB/VI implicit solvent energy function [52].

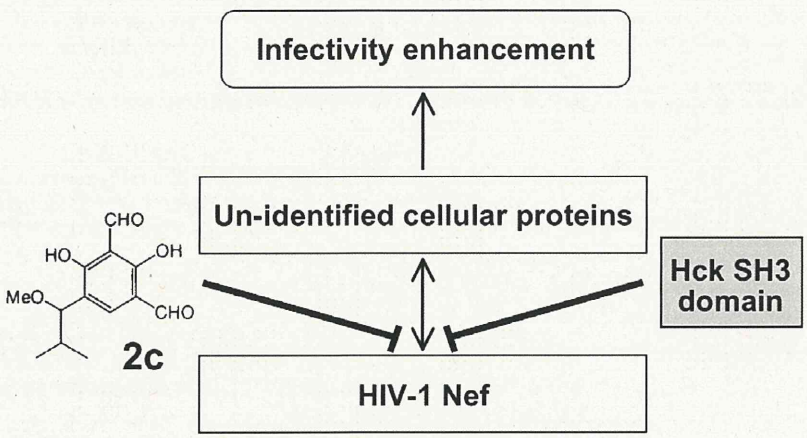

Figure 10. A model of the inhibitory effect of 2c. Both 2c and the Hck SH3 domain bind directly to Nef and reduce viral infectivity, probably by inhibiting the interaction of Nef with an unidentified cellular protein(s).
doi:10.1371/journal.pone.0027696.g010

During the docking simulation, movement of the main chain atoms around 4.5 Å of the ligand binding site in Nef was restrained with a harmonic potential of 100 kcal/mol/Å^2, while the atoms in compound 2c were not constrained. In this study, the structure with the lowest score was selected for the model.

Statistical analysis

The statistical significance of differences between assay groups was determined using Mann-Whitney U test. p values less than 0.05 were considered significant.

References

1. Fackler OT, Baur AS (2002) Live and let die: Nef functions beyond HIV replication. Immunity 16: 493–497.
2. Peterlin BM, Trono D (2003) Hide, shield and strike back: how HIV-infected cells avoid immune eradication. Nat Rev Immunol 3: 97–107.
3. Foster JL, Garcia JV (2008) HIV-1 Nef: at the crossroads. Retrovirology 5: 84.
4. Malim MH, Emerman M (2008) HIV-1 accessory proteins–ensuring viral survival in a hostile environment. Cell Host Microbe 3: 388–398.
5. Deacon NJ, Tsykin A, Solomon A, Smith K, Ludford-Menting M, et al. (1995) Genomic structure of an attenuated quasi species of HIV-1 from a blood transfusion donor and recipients. Science 270: 988–991.
6. Kirchhoff F, Greenough TC, Brettler DB, Sullivan JL, Desrosiers RC (1995) Brief report: absence of intact nef sequences in a long-term survivor with nonprogressive HIV-1 infection. N Engl J Med 332: 228–232.
7. Hanna Z, Kay DG, Rebai N, Guimond A, Jothy S, et al. (1998) Nef harbors a major determinant of pathogenicity for an AIDS-like disease induced by HIV-1 in transgenic mice. Cell 95: 163–175.
8. Garcia JV, Miller AD (1991) Serine phosphorylation-independent downregulation of cell-surface CD4 by nef. Nature 350: 508–511.
9. Schaefer MR, Wonderlich ER, Roeth JF, Leonard JA, Collins KL (2008) HIV-1 Nef targets MHC-I and CD4 for degradation via a final common β-COP-dependent pathway in T cells. PLoS Pathog 4: e1000131.
10. Schwartz O, Maréchal V, Le Gall S, Lemonnier F, Heard JM (1996) Endocytosis of major histocompatibility complex class I molecules is induced by the HIV-1 Nef protein. Nat Med 2: 338–342.
11. Greenberg ME, Iafrate AJ, Skowronski J (1998) The SH3 domain-binding surface and an acidic motif in HIV-1 Nef regulate trafficking of class I MHC complexes. EMBO J 17: 2777–2789.
12. Williams M, Roeth JF, Kasper MR, Filzen TM, Collins KL (2005) Human immunodeficiency virus type 1 Nef domains required for disruption of major histocompatibility complex class I trafficking are also necessary for coprecipitation of Nef with HLA-A2. J Virol 79: 632–637.
13. Singh RK, Lau D, Noviello CM, Ghosh P, Guatelli JC (2009) An MHC-I cytoplasmic domain/HIV-1 Nef fusion protein binds directly to the μ subunit of the AP-1 endosomal coat complex. PLoS One 4: e8364.
14. Saksela K, Cheng G, Baltimore D (1995) Proline-rich (PxxP) motifs in HIV-1 Nef bind to SH3 domains of a subset of Src kinases and are required for the enhanced growth of Nef$^+$ viruses but not for downregulation of CD4. EMBO J 14: 484–491.
15. Moarefi I, LaFevre-Bernt M, Sicheri F, Huse M, Lee CH, et al. (1997) Activation of the Src-family tyrosine kinase Hck by SH3 domain displacement. Nature 385: 650–653.
16. Lerner EC, Smithgall TE (2002) SH3-dependent stimulation of Src-family kinase autophosphorylation without tail release from the SH2 domain in vivo. Nat Struct Biol 9: 365–369.
17. Suzu S, Harada H, Matsumoto T, Okada S (2005) HIV-1 Nef interferes with M-CSF receptor signaling through Hck activation and inhibits M-CSF bioactivities. Blood 105: 3230–3237.
18. Hiyoshi M, Suzu S, Yoshidomi Y, Hassan R, Harada H, et al. (2008) Interaction between Hck and HIV-1 Nef negatively regulates cell surface expression of M-CSF receptor. Blood 111: 243–250.
19. Vérollet C, Zhang YM, Le Cabec V, Mazzolini J, Charrière G, et al. (2010) HIV-1 Nef triggers macrophage fusion in a p61Hck- and protease-dependent manner. J Immunol 184: 7030–7039.
20. Chowers MY, Spina CA, Kwoh TJ, Fitch NJ, Richman DD, et al. (1994) Optimal infectivity in vitro of human immunodeficiency virus type 1 requires an intact nef gene. J Virol 68: 2906–2914.
21. Chowers MY, Pandori MW, Spina CA, Richman DD, Guatelli JC (1995) The growth advantage conferred by HIV-1 nef is determined at the level of viral DNA formation and is independent of CD4 downregulation. Virology 212: 451–457.
22. Aiken C, Trono D (1995) Nef stimulates human immunodeficiency virus type 1 proviral DNA synthesis. J Virol 69: 5048–5056.
23. Goldsmith MA, Warmerdam MT, Atchison RE, Miller MD, Greene WC (1995) Dissociation of the CD4 downregulation and viral infectivity enhancement functions of human immunodeficiency virus type 1 Nef. J Virol 69: 4112–4121.
24. Aiken C (1997) Pseudotyping human immunodeficiency virus type 1 (HIV-1) by the glycoprotein of vesicular stomatitis virus targets HIV-1 entry to an endocytic pathway and suppresses both the requirement for Nef and the sensitivity to cyclosporin A. J Virol 71: 5871–5877.
25. Chazal N, Singer G, Aiken C, Hammarskjöld ML, Rekosh D (2001) Human immunodeficiency virus type 1 particles pseudotyped with envelope proteins that fuse at low pH no longer require Nef for optimal infectivity. J Virol 75: 4014–4018.
26. Laguette N, Benichou S, Basmaciogullari S (2009) Human immunodeficiency virus type 1 Nef incorporation into virions does not increase infectivity. J Virol 83: 1093–1104.
27. Olszewski A, Sato K, Aron ZD, Cohen F, Harris A, et al. (2004) Guanidine alkaloid analogs as inhibitors of HIV-1 Nef interactions with p53, actin, and p56lck. Proc Natl Acad Sci U S A 101: 14079–14084.
28. Emert-Sedlak L, Kodama T, Lerner EC, Dai W, Foster C, et al. (2009) Chemical library screens targeting an HIV-1 accessory factor/host cell kinase complex identify novel antiretroviral compounds. ACS Chem Biol 4: 939–947.
29. Betzi S, Restouin A, Opi S, Arold ST, Parrot I, et al. (2007) Protein protein interaction inhibition (2P2I) combining high throughput and virtual screening: Application to the HIV-1 Nef protein. Proc Natl Acad Sci U S A 104: 19256–19261.
30. Hassan R, Suzu S, Hiyoshi M, Takahashi-Makise N, Ueno T, et al. (2009) Dysregulated activation of a Src tyroine kinase Hck at the Golgi disturbs *N*-glycosylation of a cytokine receptor Fms. J Cell Physiol 221: 458–468.
31. Dikeakos JD, Atkins KM, Thomas L, Emert-Sedlak L, Byeon IJ, et al. (2010) Small molecule inhibition of HIV-1-induced MHC-I downregulation identifies a temporally regulated switch in Nef action. Mol Biol Cell 21: 3279–3292.
32. Miller MD, Warmerdam MT, Gaston I, Greene WC, Feinberg MB (1994) The human immunodeficiency virus-1 nef gene product: a positive factor for viral infection and replication in primary lymphocytes and macrophages. J Exp Med 179: 101–113.
33. Spina CA, Kwoh TJ, Chowers MY, Guatelli JC, Richman DD (1994) The importance of nef in the induction of human immunodeficiency virus type 1 replication from primary quiescent CD4 lymphocytes. J Exp Med 179: 115–123.
34. Haller C, Tibroni N, Rudolph JM, Grosse R, Fackler OT (2011) Nef does not inhibit F-actin remodelling and HIV-1 cell-cell transmission at the T lymphocyte virological synapse. Eur J Cell Biol;in press.
35. Jere A, Fujita M, Adachi A, Nomaguchi M (2010) Role of HIV-1 Nef protein for virus replication in vitro. Microbes Infect 12: 65–70.
36. Madrid R, Janvier K, Hitchin D, Day J, Coleman S, et al. (2005) Nef-induced alteration of the early/recycling endosomal compartment correlates with enhancement of HIV-1 infectivity. J Biol Chem 280: 5032–5044.
37. Tokunaga K, Kiyokawa E, Nakaya M, Otsuka N, Kojima A, et al. (1998) Inhibition of human immunodeficiency virus type 1 virion entry by dominant-negative Hck. J Virol 72: 6257–6259.
38. Choi HJ, Smithgall TE (2004) Conserved residues in the HIV-1 Nef hydrophobic pocket are essential for recruitment and activation of the Hck tyrosine kinase. J Mol Biol 343: 1255–68.
39. Rauch S, Pulkkinen K, Saksela K, Fackler OT (2008) Human immunodeficiency virus type 1 Nef recruits the guanine exchange factor Vav1 via an unexpected interface into plasma membrane microdomains for association with p21-activated kinase 2 activity. J Virol 82: 2918–2929.
40. Schindler M, Rajan D, Specht A, Ritter C, Pulkkinen K, Saksela K, et al. (2007) Association of Nef with p21-activated kinase 2 is dispensable for efficient human immunodeficiency virus type 1 replication and cytopathicity in ex vivo-infected human lymphoid tissue. J Virol 81: 13005–13014.
41. Pizzato M, Helander A, Popova E, Calistri A, Zamborlini A, et al. (2007) Dynamin 2 is required for the enhancement of HIV-1 infectivity by Nef. Proc Natl Acad Sci U S A 104: 6812–6817.
42. Bouchet J, Basmaciogullari SE, Chrobak P, Stolp B, Bouchard N, et al. (2011) Inhibition of the Nef regulatory protein of HIV-1 by a single-domain antibody. Blood 117: 3559–3568.
43. Oneyama C, Agatsuma T, Kanda Y, Nakano H, Sharma SV, et al. (2003) Synthetic inhibitors of proline-rich ligand-mediated protein-protein interaction: potent analogs of UCS15A. Chem Biol 10: 443–451.
44. Akari H, Uchiyama T, Fukumori T, Iida S, Koyama AH, et al. (1999) Pseudotyping human immunodeficiency virus type 1 by vesicular stomatitis virus G protein does not reduce the cell-dependent requirement of vif for optimal

Acknowledgments

We thank F. Koutaki for her secretarial assistance.

Author Contributions

Conceived and designed the experiments: NC SS. Performed the experiments: NC MH HO HS OF PM. Analyzed the data: NC SO SS. Contributed reagents/materials/analysis tools: TU AA. Wrote the paper: NC SS.

infectivity: functional difference between Vif and Nef. J Gen Virol 80: 2945–2959.
45. Koyanagi Y, Miles S, Mitsuyasu RT, Merrill JE, Vinters HV, et al. (1987) Dual infection of the central nervous system by AIDS viruses with distinct cellular tropisms. Science 236: 819–822.
46. Chihara T, Suzu S, Hassan R, Chutiwitoonchai N, Hiyoshi M, et al. (2010) IL-34 and M-CSF share the receptor Fms but are not identical in biological activity and signal activation. Cell Death Differ 17: 1917–1927.
47. Marti-Renom MA, Stuart AC, Fiser A, Sánchez R, Melo F, et al. (2000) Comparative protein structure modeling of genes and genomes. Annu Rev Biophys Biomol Struct 29: 291–325.
48. Baker D, Sali A (2001) Protein structure prediction and structural genomics. Science 294: 93–96.
49. Shirakawa K, Takaori-Kondo A, Yokoyama M, Izumi T, Matsui M, et al. (2008) Phosphorylation of APOBEC3G by protein kinase A regulates its interaction with HIV-1 Vif. Nat Struct Mol Biol 15: 1184–1191.
50. Grzesiek S, Bax A, Hu JS, Kaufman J, Palmer I, et al. (1997) Refined solution structure and backbone dynamics of HIV-1 Nef. Protein Sci 6: 1248–63.
51. Wang J, Cieplak P, Kollman PA (2000) How well does a restrained electrostatic potential (RESP) model perform in calcluating conformational energies of organic and biological molecules? J Comput Chem 21: 1049–1074.
52. Labute P (2008) The generalized Born/volume integral implicit solvent model: estimation of the free energy of hydration using London dispersion instead of atomic surface area. J Comput Chem 29: 1693–1698.
53. Goto J, Kataoka R, Muta H, Hirayama N (2008) ASEDock-docking based on alpha spheres and excluded volumes. J Chem Inf Model 48: 583–90.
54. Halgren TA (1999) MMFF VII. Characterization of MMFF94, MMFF94s, and other widely available force fields for conformational energies and for intermolecular-interaction energies and geometries. J Comput Chem 20: 720–29.
55. Halgren TA (1999) MMFF VI. MMFF94s option for energy minimization studies. J Comput Chem 20: 730–48.

Molecular Biology of the Cell
Vol. 21, 3279–3292, October 1, 2010

Small Molecule Inhibition of HIV-1–Induced MHC-I Down-Regulation Identifies a Temporally Regulated Switch in Nef Action

Jimmy D. Dikeakos,*# Katelyn M. Atkins,*# Laurel Thomas,* Lori Emert-Sedlak,† In-Ja L. Byeon,‡ Jinwon Jung,‡ Jinwoo Ahn,‡ Matthew D. Wortman,§ Ben Kukull,‖ Masumichi Saito,¶ Hirokazu Koizumi,¶ Danielle M. Williamson,* Masateru Hiyoshi,¶ Eric Barklis,‖ Masafumi Takiguchi,¶ Shinya Suzu,¶ Angela M. Gronenborn,‡ Thomas E. Smithgall,† and Gary Thomas*

*Vollum Institute, Oregon Health & Science University, Portland, OR 97239; Departments of †Microbiology and Molecular Genetics and ‡Structural Biology, University of Pittsburgh, PA 15260; §Drug Discovery Center, University of Cincinnati, OH 45237; ‖Department of Molecular Microbiology and Immunology, Oregon Health & Science University, Portland, OR 97239; ¶Center for AIDS Research, Kumamoto University, Kumamoto, Japan 860-0811

Submitted May 28, 2010; Revised July 29, 2010; Accepted July 30, 2010
Monitoring Editor: Howard Riezman

HIV-1 Nef triggers down-regulation of cell-surface MHC-I by assembling a Src family kinase (SFK)-ZAP-70/Syk-PI3K cascade. Here, we report that chemical disruption of the Nef-SFK interaction with the small molecule inhibitor 2c blocks assembly of the multi-kinase complex and represses HIV-1–mediated MHC-I down-regulation in primary CD4$^+$ T-cells. 2c did not interfere with the PACS-2–dependent trafficking of Nef required for the Nef-SFK interaction or the AP-1 and PACS-1–dependent sequestering of internalized MHC-I, suggesting the inhibitor specifically interfered with the Nef-SFK interaction required for triggering MHC-I down-regulation. Transport studies revealed Nef directs a highly regulated program to down-regulate MHC-I in primary CD4$^+$ T-cells. During the first two days after infection, Nef assembles the 2c-sensitive multi-kinase complex to trigger down-regulation of cell-surface MHC-I. By three days postinfection Nef switches to a stoichiometric mode that prevents surface delivery of newly synthesized MHC-I. Pharmacologic inhibition of the multi-kinase cascade prevents the Nef-dependent block in MHC-I transport, suggesting the signaling and stoichiometric modes are causally linked. Together, these studies resolve the seemingly controversial models that describe Nef-induced MHC-I down-regulation and provide new insights into the mechanism of Nef action.

INTRODUCTION

After infection by HIV-1, the acute viremia induces an immune response that includes the development of anti-HIV CD8$^+$ cytotoxic T lymphocytes (CTLs) (Gandhi and Walker, 2002). Though a significant number of the circulating CTL population is directed against HIV-1–infected cells, the virus escapes the adaptive immune response, establishing reservoirs in numerous cell types that can resist highly active antiretroviral therapy (HAART) (Stevenson, 2003). During disease progression, the HIV-1 viral load increases greatly, destroying most of the CD4$^+$ lymphocytes, leaving patients increasingly susceptible to opportunistic infections (Douek *et al.*, 2003).

The adaptive immune response requires members of the class I major histocompatibility complex (MHC-I) to present viral antigens on the surface of infected cells, which destroys the infected cell by the cytolytic, apoptosis-inducing actions of CTLs (Lieberman, 2003). Large DNA viruses, including herpesviruses and poxviruses, possess a large collection of immune evasive genes that are expressed in a coordinated manner to target nearly every step in the biosynthesis, assembly, transport, and cell-surface localization of MHC-I molecules (Yewdell and Hill, 2002; Peterlin and Trono, 2003). By contrast, HIV-1 relies on the single 27-kDa N-myristoylated early gene product Nef to down-regulate MHC-I (Peterlin and Trono, 2003). Nef is required for the onset of AIDS and can affect cells in many ways, including alteration of T-cell activation and maturation, subversion of the apoptotic machinery, and the down-regulation of cell-surface molecules, notably CD4 and MHC-I (Fackler and Baur, 2002). Down-regulation of CD4 through the clathrin/AP-2 pathway to lysosomes eliminates interference of the viral receptor with HIV-1 envelopment or release. Down-regula-

This article was published online ahead of print in *MBoC in Press* (http://www.molbiolcell.org/cgi/doi/10.1091/mbc.E10–05–0470) on August 4, 2010.

# These authors contributed equally to this work.

Address correspondence to: Gary Thomas (thomasg@ohsu.edu).

tion of cell-surface MHC-I molecules encoded by the HLA-A and -B loci to paranuclear TGN/endosomal compartments mediates the ability of HIV-1 to evade the $CD8^+$ immune surveillance system (Blagoveshchenskaya *et al.*, 2002; Tomiyama *et al.*, 2002; Yang *et al.*, 2002; Peterlin and Trono, 2003).

Two models—here referred to as the "signaling" and "stoichiometric" down-regulation pathways—are currently used to explain the molecular basis of Nef-mediated MHC-I down-regulation (see Hung *et al.*, 2007). The "signaling" model describes the sequential roles of three conserved Nef sites in mediating MHC-I down-regulation. The pathway is initiated by the $EEEE_{65}$-dependent binding to the sorting protein PACS-2, which targets Nef to the paranuclear region, enabling $PXXP_{75}$ to bind and activate a Golgi region-localized Src Family Kinase (SFK). This Nef-SFK complex then phosphorylates ZAP-70 (Syk in monocytes and heterologous cells), forming a phosphotyrosine-based docking motif that recruits class I PI3K by ligating the p85 regulatory subunit C-terminal SH2 domain. This multi-kinase complex then triggers internalization of cell-surface MHC-I through a clathrin-independent, ARF6-dependent pathway (Blagoveshchenskaya *et al.*, 2002; Hung *et al.*, 2007; Atkins *et al.*, 2008). After internalization, Nef M_{20}, located within an amphipathic α-helix, mediates the sequestering of endocytosed MHC-I molecules into paranuclear compartments (Blagoveshchenskaya *et al.*, 2002; Hung *et al.*, 2007; Chaudhry *et al.*, 2008). By contrast, the "stoichiometric" model envisions that Nef mediates MHC-I down-regulation by acting solely via a PI3K-independent pathway that diverts newly synthesized MHC-I molecules to degradative compartments by an M_{20}- and AP-1–dependent mechanism (Kasper and Collins, 2003; Roeth *et al.*, 2004; Kasper *et al.*, 2005). However, an alternative interpretation of the stoichiometric model suggests Nef binds endocytosed MHC-I but the underlying mechanism was not described (Roeth *et al.*, 2004; Noviello *et al.*, 2008). While the stoichiometric model suggests the importance of Nef M_{20} in mediating MHC-I down-regulation—a finding consistent with both models—it fails to address the roles of $EEEE_{65}$ and the $PXXP_{75}$ site within the polyproline helix.

The binding of HIV-1 Nef to the SH3 domains of SFKs requires $PXXP_{75}$ and an adjacent hydrophobic pocket, which anchors the SFK on Nef (Lee *et al.*, 1995). The determination that Nef can bind and directly activate a subset of SFKs together with the conservation of the SH3 domain binding site across various Nef alleles (Choi and Smithgall, 2004; Trible *et al.*, 2006) suggests the Nef-SFK interaction is required for disease progression, including AIDS-like disease in animal models and assembly of the SFK-ZAP-70/Syk-PI3K multi-kinase complex, which triggers MHC-I down-regulation in primary $CD4^+$ T-cells and promonocytic cells (Hanna *et al.*, 1998; Hung *et al.*, 2007). These findings suggest that targeting the assembly of the multi-kinase complex may represent an attractive approach to inhibiting AIDS progression. The ability of isoform-specific class I PI3K kinase inhibitors to repress Nef-induced MHC-I down-regulation in primary $CD4^+$ T-cells supports this possibility (Hung *et al.*, 2007; Atkins *et al.*, 2008). Alternatively, small molecule inhibitors that disrupt the binding of Nef to one or more of the kinases that form the multi-kinase complex would inhibit Nef action without disrupting the activity of cellular kinases that may be required for host cell function.

Here we report that small molecule disruption of Nef-SFK binding represses MHC-I down-regulation in HIV-1–infected primary $CD4^+$ T-cells by interfering with formation of the multi-kinase complex. We further show that Nef-induced MHC-I down-regulation in primary $CD4^+$ T-cells is manifest by the sequential action of the signaling mode, which lasts for more than two days after infection, followed by the stoichiometric mode by three days postinfection. Interference with the multi-kinase complex that triggers the signaling mode disrupts the subsequent stoichiometric block in MHC-I transport, suggesting the two modes are causally linked. These studies challenge the current dogma of Nef-mediated MHC-I down-regulation (Hansen and Bouvier, 2009) and suggest Nef orchestrates a highly regulated molecular program consisting of the sequential use of signaling followed by stoichiometric modes to evade immune surveillance.

MATERIALS AND METHODS

Cells, Viruses, and Plasmids

293T, A7, BSC-40, HeLa-$CD4^+$, H9 $CD4^+$ T-cells, and CEM T-cells were cultured as described (Hung *et al.*, 2007). Peripheral blood was obtained from healthy HLA-A^*0201^+ volunteers by leukapheresis or venipuncture using protocols approved by the OHSU Institutional Review Board (protocols IRB00004039 and IRB00002251) or by the International Medical Center of Japan and the Kumamoto University Ethical Committee. Primary human $CD4^+$ T-cells were isolated as described (Hung *et al.*, 2007) and cultured in RPMI 1640 containing 10% FBS and supplemented with IL-2 (50 U/ml; Sigma) and 1 μg/ml PHA (Sigma, St. Louis, MO) before infection. HIV-1^{NL4-3}, vaccinia virus (VV), and vaccinia recombinants expressing FLAG-tagged Nef (Nef/f, C-terminal epitope tag), Nef_{AXXA}/f, Nef_{AXXA}-PI3K*, Hck, Src, or ZAP-70, and HIV pseudotyped viruses NL4-3ΔG/P-EGFP (titer = 4.5×10^7 IFU/ml) and NL4-3ΔG/P-EGFP/ΔNef (titer = 2.1×10^7 IFU/ml) were grown and titered by marker expression as described (Blagoveshchenskaya *et al.*, 2002; Hung *et al.*, 2007). Adenoviruses expressing HA-tagged PACS-1 or PACS-2 were described previously (Blagoveshchenskaya *et al.*, 2002; Simmen *et al.*, 2005). Nef-eYFP, Nef_{AXXA}-eYFP and pPTEN were previously described (Hung *et al.*, 2007) and pmaxGFP was obtained from Dharmacon (Boulder, CO).

Inhibitors, siRNAs, qRT-PCR, and Kinase Assays

PI-103 (Calbiochem, San Diego, CA) and 2c (2,4-dihydroxy-5-(1-methoxy-2-methylpropyl)benzene-1,3-dialdehyde, (Kyowa Hakko Kirin Co., Tokyo, Japan) were used as indicated. 2c toxicity was determined by MTT (Invitrogen, Carlsbad, CA) according to manufacturer's instructions. Control (nonspecific) siRNA and siRNAs specific for Hck, Lyn, Src, PACS-1, PACS-2, or the μ1A subunit of AP-1 (Smartpool, Dharmacon) were nucleofected (Amaxa, Gaithersburg, MD) into cells according to manufacturer's instructions. RNA was purified from H9 cells nucleofected with siRNAs as indicated in figure legends using the RNeasy kit (Qiagen, Valencia, CA) according to manufacturer's instructions. cDNA was reverse transcribed from RNA using the random decamers from the RETROscript Kit (Ambion, Austin, TX) via manufacturer's instructions. Utilizing commercially-available Hck, Lyn, and Src primers (Qiagen) and SYBR green qPCR reagent (SA-Biosciences, Frederick, MD), q-PCR was conducted on a StepOnePlus Real-time PCR system (Applied Biosciences, Foster City, CA). PI3K assays were performed as described (Atkins *et al.*, 2008). In vitro Hck kinase assays were performed as described (Emert-Sedlak *et al.*, 2009).

Flow Cytometry and Immunofluorescence Microscopy

For flow cytometry, cells were processed as described (Hung *et al.*, 2007; Atkins *et al.*, 2008) and stained using the following antibodies: anti-MHC-I (W6/32), anti-HLA-A2 (BB7.2, BD, San Jose, CA), anti-CD4-APC (Biolegend, San Diego, CA), or anti-p24-FITC (Virostat, Portland, ME) as indicated in legends. PE-conjugated donkey anti-mouse IgG (Jackson IR, West Grove, PA) was used to stain MHC-I– and HLA-A2–positive cells. Isotype-matched antibodies (Serotec, Raleigh, NC) were used as negative controls. Samples were processed on a FACSCalibur (BD) as described (Atkins *et al.*, 2008) and data analyzed using FCS express (De Novo Software, Los Angeles, CA). For immunofluorescence microscopy, cells were processed as indicated in legends and processed for immunofluorescence as described (Atkins *et al.*, 2008). Confocal images were captured as described (Atkins *et al.*, 2008) and colocalization of Nef-eYFP with Golgin-97 was quantified morphometrically using Imaris 7.0. A mask for each field of cells was generated based on the fluorescent signal of Golgin-97 and the percent colocalization of Golgin-97 with Nef-eYFP was determined and presented as the mean $\pm$ SD from at least 20 cells per condition.

Immunoprecipitation, Western Blot, and Antibody Uptake

Cells infected with the indicated VV recombinants were harvested as described (Atkins *et al.*, 2008). Where indicated, cells were treated with the

corresponding concentration of 2c before harvest. Flag-tagged Nef constructs were immunoprecipitated with mAb M2-agarose (Sigma), and associated proteins were detected by Western blot. The following antibodies were obtained as indicated: mAb HA.11 (Covance, San Diego, CA); anti-Hck, anti-Lyn (Santa Cruz, Santa Cruz, CA); anti-p85, anti-Src, anti-ZAP-70 (Upstate, Bedford, MA); anti-phospho$_{292}$ZAP-70 (BD); anti-Akt, anti-pAkt, anti-His$_6$, anti-PTEN, anti-cleaved caspase-3 (Cell Signaling, Danvers, MA); anti-actin (Chemicon, Bedford, MA); anti-Nef #2949 (obtained through NIH AIDS Research and Reference Reagent Program), anti-MHC-I K455 (provided by K. Früh, OHSU), W6/32 and HC10 (provided by D. Johnson, OHSU); anti-AP-1 μ1A subunit (provided by L. Traub, University of Pittsburgh), AP-γ1 (Sigma), anti-PACS-1 (703), anti-PACS-2 (Atkins *et al.*, 2008). Antibody uptake using mAb W6/32 was performed as described (Blagoveshchenskaya *et al.*, 2002).

NMR Spectroscopy

The cDNA encoding consensus *nef* (obtained from the NIH AIDS Research and Reference Reagent Program) was His$_6$-tagged, inserted into pET21 vector (EMD chemicals, San Diego, CA), and protein was expressed in Rosetta 2 (DE3) *E. coli*, cultured in modified minimal medium using $^{15}NH_4Cl$ as the sole nitrogen source, and induced with 0.4 mM IPTG at 18°C for 16 h. Soluble forms of His$_6$-tagged Nef proteins were purified over a Ni^{+2}-NTA column (GE Healthcare, Uppsala, Sweden) and subsequent gel-filtration on a Superdex200 26/60 column (GE Healthcare) equilibrated with 25 mM sodium phosphate buffer (pH 7.5), 150 mM NaCl, 1 mM DTT, and 0.02% sodium azide. Two-dimensional (2D) ^1H-^{15}N heteronuclear single quantum coherence (HSQC) experiments (Bodenhausen and Ruben, 1980) were performed at 27°C on a Bruker Avance 700 MHz spectrometer equipped with a 5-mm, triple resonance, and *z*-axis gradient cryoprobe. The ^1H-^{15}N HSQC spectrum of free Nef was obtained using a 80-μM uniform ^{15}N-labeled Nef sample in 10 mM HEPES, 10 mM DTT, 100 mM NaCl, and 5% (vol/vol) D_2O (pH 8.0). A series of ^1H-^{15}N HSQC spectra were acquired to monitor chemical shift changes upon addition of aliquots of a 10-mM 2c stock solution, dissolved in DMSO, to the Nef sample. The Nef:2c molar ratios of the solutions were 1:0, 1:0.6, 1:1.75, 6.25, and 12.5. A control series of ^1H-^{15}N HSQC spectra were also obtained after adding the same amounts of DMSO without 2c to the free Nef sample. In this series, in contrast to the titration with the 2c solution, minimal spectral changes occurred (data not shown), confirming that the changes after addition of 2c were indeed caused by this organic molecule and not the solvent.

Transport Assay and Endo H Treatment

H9 cells were infected with Nef^- or Nef^+ pseudotyped HIV-1^{NL4-3} viruses for 24, 48, or 72 h. After infection, cells were subjected to pulse-chase/surface biotinylation as described (Blagoveshchenskaya *et al.*, 2002). Briefly, to IP with HC10, cells were lysed in m-RIPA [1% NP-40, 1% sodium deoxycholate, 150 mM NaCl, 50 mM Tris-HCl (pH 8.0)] and then heated for 1 h at 55°C to denature MHC-I proteins. To IP with BB7.2, cells were lysed in PBS (pH 7.2) containing 1% NP-40. Bound MHC-I proteins were eluted from protein A sepharose beads (Sigma) by boiling in TBS, 5% SDS, 2% NP-40, and 2% sodium deoxycholate. One-third of the eluate was used to assess total MHC-I while the rest was incubated with streptavidin agarose (Pierce, Rockford, IL) to capture biotinylated MHC-I. For Endo H treatment, MHC-I was eluted by boiling in 10 mM Tris-HCl (pH 7.4) containing 1% SDS, precipitated with acetone and resuspended in glycoprotein denaturation buffer (NEB, Ipswich, MA) and digested with 10 U of Endoglycosidase H for 1 h at 37°C. Samples were separated by SDS-PAGE and processed using Amplify (GE Healthcare). Quantification was performed using NIH Image J.

Protein Interaction Assays

Plasmids expressing GST, GST-MHC-I CDNef$_{LL/AA}$ (provided by J. Guatelli, UCSD), His$_6$-HcK$\wedge$OR GST-Nef (strain NL4-3), were transformed in BL21 *E. coli* and cultures were induced with 1 mM IPTG (Calbiochem) for 4 h at 37°C. Bacterial pellets were resuspended in lysis buffer [50 mM Tris (pH 7.6), 1.5 mM EDTA, 100 mM NaCl, 0.5% Triton X-100, 0.1 mM DTT, 10 mM $MgCl_2$] containing protease inhibitors (0.5 mM PMSF and 0.1 μM each of aprotinin, E-64, and leupeptin), lysed using a French Press (Aminco, Rockville, MD) and incubated with GST-sepharose (GE Healthcare). For the interaction with GST-MHC-I CDNef$_{LL/AA}$, A7 cells were lysed in 50 mM Tris-HCl (pH 8.0), 1% Triton X-100, 5 mM EDTA, 150 mM NaCl, 10 mM $MgCl_2$ with protease inhibitors (0.5 mM PMSF and 0.1 μM each of aprotinin, E-64, and leupeptin). A7 lysates were added to GST-Sepharose bound to the proteins of interest overnight at 4°C. The resin was incubated or not with 20 μM 2c for one hour, washed three times in lysis buffer and once in 50 mM Tris (pH 8.0), and resuspended in SDS-PAGE sample buffer. For the His$_6$-Hck interaction with GST-Nef, the proteins were mixed at a 2:1 ratio (Hck:Nef) for 30 min at 4°C in binding buffer [0.1% NP-40, 0.1 mM EDTA, 20 mM Tris (pH 7.9), 150 mM NaCl] containing the indicated concentrations of 2c. After incubation, GST-Sepharose was added and subsequently washed three times in binding buffer and resuspended in SDS-PAGE sample buffer.

RESULTS

HIV-1 Nef Uses a Subset of SFKs to Trigger MHC-I Down-Regulation

Formation of the SFK-ZAP70/Syk-PI3K multi-kinase complex is initiated by the PXXP$_{75}$-dependent binding of Nef to the SH3 domain of a Golgi region-localized SFK, directly activating the kinase (Hung *et al.*, 2007). Of the seven known SFKs only a subset—Hck, Lyn, and Src—can be directly activated after Nef binding and are found in the Golgi region, suggesting one or more of these kinases mediate MHC-I down-regulation (Matsuda *et al.*, 2006; Trible *et al.*, 2006; Hiyoshi *et al.*, 2008; Pulvirenti *et al.*, 2008). To test this, H9 $CD4^+$ T-cells treated with siRNAs specific for Hck, Lyn, or Src (Figure 1A and supplemental Figure S1) were infected with recombinant viruses expressing Nef and the extent of MHC-I down-regulation was determined. Nef-induced MHC-I down-regulation was slightly repressed by siRNA knockdown of Hck alone but blocked by knockdown of Hck, Lyn, and Src together. The data suggest that Hck, Lyn, and Src function redundantly in Nef-induced MHC-I down-regulation.

Small Molecule Inhibition of the Nef-SFK Interaction

The determination that Nef assembles a multi-kinase complex to trigger MHC-I down-regulation suggests this pathway can be selectively targeted pharmacologically. Indeed, isoform-specific class I PI3K inhibitors repress Nef-induced MHC-I down-regulation in primary $CD4^+$ T-cells (Hung *et al.*, 2007; Atkins *et al.*, 2008). An alternative approach would be to block protein-protein interactions required for complex assembly without affecting cellular enzyme activity directly. The characterized binding of Nef to SFK SH3 domains represents an ideal target for this type of inhibitor (Arold *et al.*, 1997). One candidate compound, 2c (supplemental Figure S2), is a derivative of the compound UCS15A that disrupts the PXXP-dependent binding of Sam68 to Src (Oneyama *et al.*, 2003). To test whether 2c disrupts Nef-SFK binding, we treated H9 $CD4^+$ T-cells coexpressing flag-tagged Nef (Nef/f) and Hck with increasing concentrations of 2c. Hck was used because it binds Nef with higher affinity than other SFKs and Nef can assemble Hck into the multi-kinase complex (Hung *et al.*, 2007; Atkins *et al.*, 2008). Coimmunoprecipitation analysis showed 2c repressed the interaction between Nef and Hck in a dose-dependent manner as well as repressed the interaction with Lyn or Src (Figure 1B and supplemental Figure S3). Next, we incubated GST-Nef and His$_6$-Hck with increasing concentrations of 2c and found that 2c disrupted Nef-Hck binding in a dose-dependent manner (Figure 1C). To determine whether the ability of 2c to inhibit Nef-SFK binding also blocked Nef-induced SFK activation, we incubated recombinant, purified Nef, and Hck with increasing concentrations of 2c and measured the resulting Nef-induced Hck activity using a FRET-based in vitro kinase assay. Under these assay conditions, activation of Hck is dependent upon Nef (Emert-Sedlak *et al.*, 2009). As shown in Figure 1D, 25 μM 2c substantially repressed Nef-dependent Hck activity without affecting Hck in the absence of Nef. High 2c concentrations ($\geq$100 μM), however, directly inhibited Hck activity. These findings suggest 2c has a bimodal effect on Hck activity; at low concentrations 2c disrupts Nef-induced kinase activity, whereas high concentrations of 2c inhibit Hck directly.

The ability of 2c to selectively inhibit Nef-induced Hck activation suggested 2c may bind Nef directly, thereby affecting Hck activity. Accordingly, ^1H-^{15}N HSQC NMR analysis of the interaction of 2c with recombinant Nef in solution revealed 2c

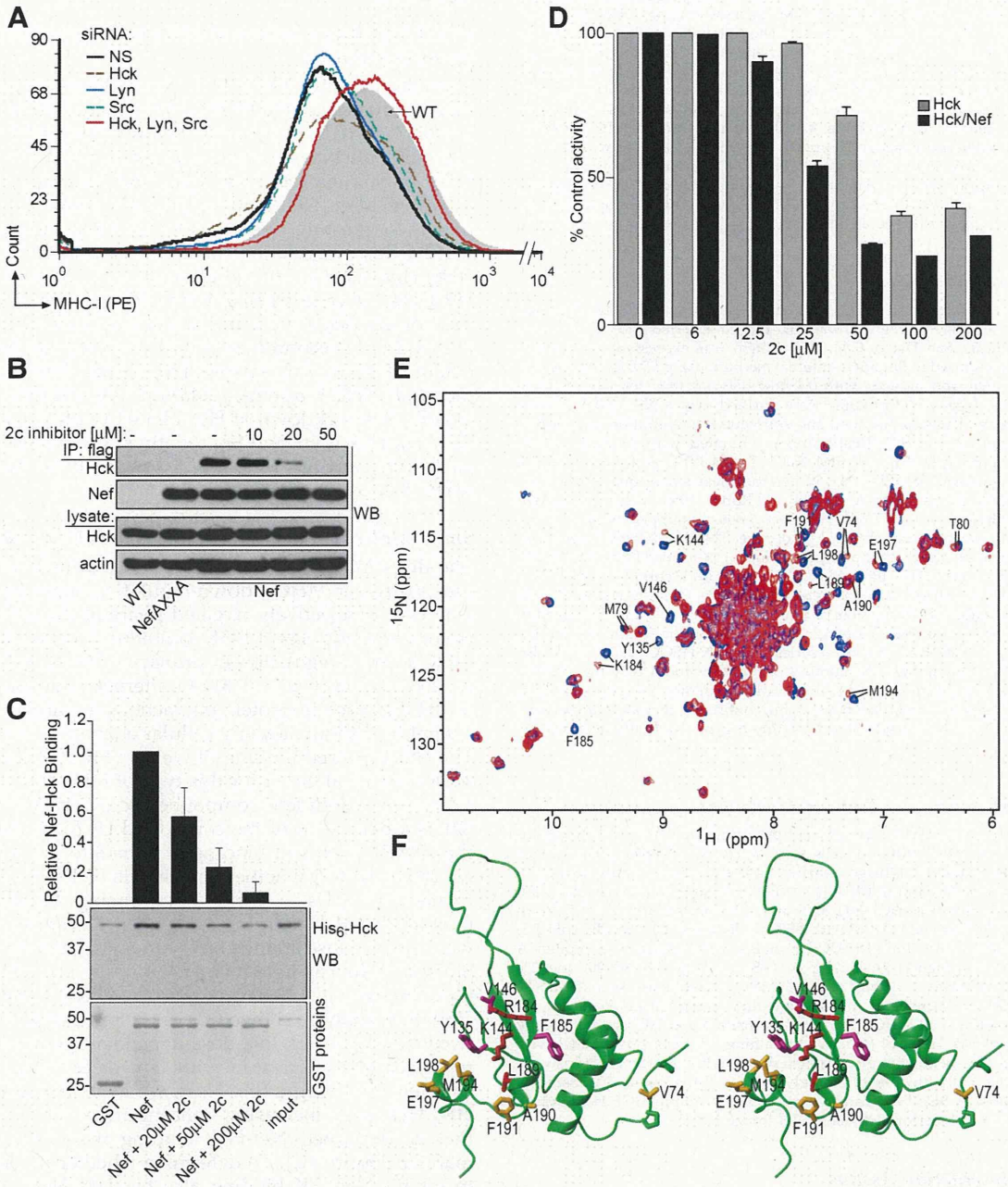

Figure 1. 2c interferes with Nef:SFK binding. (A) H9 CD4$^+$ T-cells were nucleofected (Amaxa) on days 1 and 3 with pmaxGFP and nonspecific siRNA or siRNAs that target Hck, Lyn, or Src alone or in combination. On day 4 cells were infected with VV:WT (gray filled) or VV:Nef (lines, unfilled) (moi = 10, 8 h), and analyzed by flow cytometry using mAb W6/32 as described in experimental procedures. MFI: NS siRNA (WT = 167, Nef = 99.5); Nef + Hck siRNA = 120; + Lyn siRNA = 103; + Src siRNA = 117; + Hck, Lyn, Src = 169. MFI, mean fluorescence intensity. (B) H9 cells were coinfected with VV:WT, VV:Nef/f or Nef_{AXXA}/f (moi = 10, 8 h) and VV:Hck (moi = 2, 8 h) and treated with 10, 20, or 50 μM 2c for 4 h before harvest. Nef/f proteins were immunoprecipitated, and coprecipitating Hck was detected by Western blot. (C) GST-Nef was incubated with His_6-Hck and treated with increasing concentrations of 2c. GST-Nef was captured, and bound His_6-Hck was quantified using NIH Image J. Accordingly, nonspecific binding of GST to His_6-Hck was subtracted and values were normalized to the binding of GST-Nef to His_6-Hck in the absence of 2c. Each condition was assayed in triplicate, and results are presented as the mean ± SD. (D) Hck alone (gray bars) or Hck plus Nef (black bars) were treated with increasing concentrations of 2c. The resulting Hck enzyme activity was measured using a fluorometric assay and expressed relative to 100% control activity. Each condition was assayed in quadruplicate and results are presented as the mean ± SD. (E) Superposition of ^{1}H-^{15}N HSQC spectra of Nef in the absence (blue) and presence (red) of 2c. The ^{1}H-^{15}N HSQC spectra were recorded on 80 μM uniform ^{15}N-labeled Nef samples at 27°C in the absence (blue) and presence (red) of 1 mM 2c (1:12.5 M ratio of Nef to 2c). All assignable amide resonances (J. Jung, I.-J.L. Byeon, J. Ahn, and A.M. Gronenborn, unpublished data) that exhibit chemical shift changes >0.06 ppm are labeled with residue name and number. The resonances of Y_{135}, V_{146}, and F_{185} are labeled only on the free Nef spectrum because the identification of the bound resonances was not straightforward either due to very large shift changes or severe line broadening beyond detection. The resonances of M_{79} ($\Delta\delta$ = 0.041ppm) and T_{80} ($\Delta\delta$ = 0.025ppm), which are located immediately after the $P_{72}XXP_{75}$ motif, are also labeled. Concentrations of 2c as low as 48 μM, representing a 1:0.6 M ratio of Nef

induces a number of chemical shift changes in amide resonances of Nef (Figure 1E). These include relatively small chemical shift changes (0.025–0.063ppm) at V_{74}, M_{79}, and T_{80} located within the Nef polyproline helix that binds the RT loop of SH3 domains on SFKs (Lee *et al.*, 1995), suggesting 2c may influence the conformation of the polyproline helix. The presence of resonance overlap in the NMR spectra precluded more detailed analysis involving the disordered regions of Nef such as the N-terminal region preceding the polyproline helix and the internal loop consisting of residues E_{149}–K_{178}. More pronounced chemical shift changes (>0.1ppm) were observed for the resonances of Y_{135}, K_{144}, V_{146}, K_{184} (R_{184} in Figure 1F [PDB ID:2NEF]), F_{185}, and L_{189} which are clustered on the opposite side of the SH3 domain binding site. Other residues in this region such as V_{148}, A_{190}, F_{191}, M_{194}, and E_{197}, and L_{198} also undergo substantial (>0.06ppm) changes. These chemical shift perturbations caused by the addition of 2c imply that 2c could bind to the cleft formed by the central β-sheet and the C-terminal α-helices of Nef, which may provide a good binding pocket (Figure 1F). Together, these findings suggest 2c may interfere with Nef-induced SFK activation most likely by allosteric inhibition of SFK binding or possibly by directly influencing the binding mode of the polyproline helix to SFKs or both.

2c Represses the Ability of HIV-1 to Down-Regulate MHC-I

The 2c concentration range that selectively inhibited Nef-dependent SFK activation showed no measurable cell toxicity up to 60 μM for two days, suggesting 2c could be tested in culture (Figure S4, panel A). Accordingly, we treated H9 cells expressing Nef-eYFP with 2c or the class I PI3K inhibitor PI-103, which specifically blocks Nef-induced MHC-I down-regulation (Hung *et al.*, 2007), and measured cell-surface MHC-I (Figure 2A). In agreement with earlier studies (Hung *et al.*, 2007; Atkins *et al.*, 2008), Nef-eYFP induced an ~twofold down-regulation of MHC-I that was blocked by PI-103. Similarly, 2c partially blocked MHC-I down-regulation. Next, we asked whether 2c could interfere with HIV-1–induced MHC-I down-regulation in primary $CD4^+$ T-cells. We infected primary $CD4^+$ T-cells with HIV-1^{NL4-3} and treated the cultures with vehicle or 2c. At 8 d postinfection, the cells were analyzed for cell-surface HLA-A2 and CD4 by flow cytometry (Figure 2B). We found that 2c partially blocked down-regulation of MHC-I but had no effect on down-regulation of CD4, which is mediated by a class I PI3K-independent pathway (Hung *et al.*, 2007).

2c Disrupts Formation of the Multi-Kinase Complex

The ability of 2c to disrupt Nef-SFK binding as well as HIV-1–induced MHC-I down-regulation suggested this compound would disrupt assembly of the SFK-ZAP-70-PI3K multi-kinase complex. Accordingly, we found that 2c blocked the ability of Nef to recruit class I PI3K activity using an in vitro lipid kinase assay (Figure 3A). Moreover, this result was not due to cell toxicity or induction of apoptosis nor was it due to nonspecific inhibition of class I PI3K as treatment of the immunoprecipitate with 40 μM 2c had no effect on enzyme activity (supplemental Figure S4, B and C and Figure 3A). The titration analysis of 2c on Nef-induced Hck activation (Figure 1D) suggests 40 μM 2c blocked Nef-induced PI3K stimulation by selective inhibition of Nef-induced SFK activation, whereas 100 μM 2c may block Nef-induced PI3K stimulation by additionally inhibiting SFK activation directly. The PI3K activity results were supported by coimmunoprecipitation analysis in which 2c inhibited formation of the multi-kinase complex by disrupting the interaction of Nef with Hck, phospho-ZAP-70 and the class I PI3K p85 regulatory subunit (Figure 3B).

The ability of 2c to disrupt Nef-SFK binding did not exclude the possibility that it may affect additional steps in the MHC-I down-regulation pathway. We first asked whether 2c interfered with steps upstream of Nef-SFK binding. Accordingly, we found that 2c had no effect on the Nef-PACS-2 interaction nor the PACS-2–dependent trafficking of Nef-eYFP to the paranuclear region, which is required for Nef-SFK binding and Nef-induced MHC-I down-regulation (Figure 3, C and D and Atkins *et al.*, 2008).

Because Nef M_{20} mediates the interaction with AP-1 (Roeth *et al.*, 2004) and is essential for sequestration of MHC-I molecules after their internalization from the cell surface (Blagoveshchenskaya *et al.*, 2002), we tested whether AP-1 was required in the last stage of this signaling pathway. Accordingly, H9 cells knocked down for AP-1A, PACS-2, or PACS-1 which is required for MHC-I down-regulation but not for triggering PI3K stimulation (Piguet *et al.*, 2000; Atkins *et al.*, 2008), were infected with viruses expressing Nef or the Nef_{AXXA}-PI3K* chimera, which rescues the inability of Nef_{AXXA} to down-regulate MHC-I by overriding the requirement for assembly of the SFK-ZAP-70-PI3K complex (supplemental Figure S5 and Blagoveshchenskaya *et al.*, 2002; Hung *et al.*, 2007). The ability of Nef or Nef_{AXXA}-PI3K* to down-regulate MHC-I in cells knocked down for expression of PACS-2, PACS-1, or AP-1A was assessed by antibody uptake to discern the importance of each protein in steps upstream or downstream of PI3K stimulation (Figure 4A). Consistent with our determination that Nef requires PACS-2 upstream of PI3K (Atkins *et al.*, 2008), siRNA knockdown of PACS-2 blocked MHC-I uptake by Nef but not by Nef_{AXXA}-PI3K*. By contrast, siRNA knockdown of AP-1A or PACS-1 blocked MHC-I uptake induced by Nef and Nef_{AXXA}-PI3K*, demonstrating AP-1 and PACS-1 act downstream of PI3K stimulation.

To test potential effects of 2c on the later stages of this pathway, we asked whether 2c interfered with the interaction between Nef and PACS-1 or AP-1. We determined that 2c had no effect on the Nef-PACS-1 interaction (Figure 4B). Additionally, the interaction of AP-1 with Nef M_{20} and the MHC-I cytosolic domain can be recapitulated using the chimeric protein GST-MHC-I CD-$Nef_{LL/AA}$ to capture AP-1 from cytosol preparations (Noviello *et al.*, 2008). This chimera consists of Nef with an $LL_{165}\rightarrow AA$ substitution, which blocks the LL_{165}-dependent binding to adaptors, fused to the MHC-I cytosolic domain. We found that 2c did not interfere with the ability of GST-MHC-I CD-$Nef_{LL/AA}$ to capture AP-1 (Figure 4C, left). Interest-

Figure 1 (cont). to 2c, revealed chemical shift changes between ^{15}N-Nef and 2c. (F) Structural mapping of the chemical shift changes in the ^{1}H-^{15}N HSQC spectrum of Nef induced by 2c onto the Nef NMR structure (PDB ID: 2NEF, see (Grzesiek *et al.*, 1997)). The ^{1}H-^{15}N-combined chemical shift changes were calculated using $\sqrt{\Delta\delta_{HN}{}^2+(\Delta\delta_N\times 0.1)^2}$, with $\Delta\delta_{HN}$ and $\Delta\delta_N$ the ^{1}HN and ^{15}N chemical shift differences, respectively, between the free and 2c-bound Nef protein spectrum. On a stereoview of the structure in ribbon representation, sidechains of residues whose amide resonances exhibit significant changes are shown in stick representation and color coded according to the size of the change: orange; 0.06–0.1 ppm, and red; >0.1 ppm. Residues whose ^{1}H-^{15}N HSQC amide resonances are only detectable/assignable in free Nef are colored in magenta and the sidechains of the two prolines in the $P_{72}XXP_{75}$ region are shown in green.

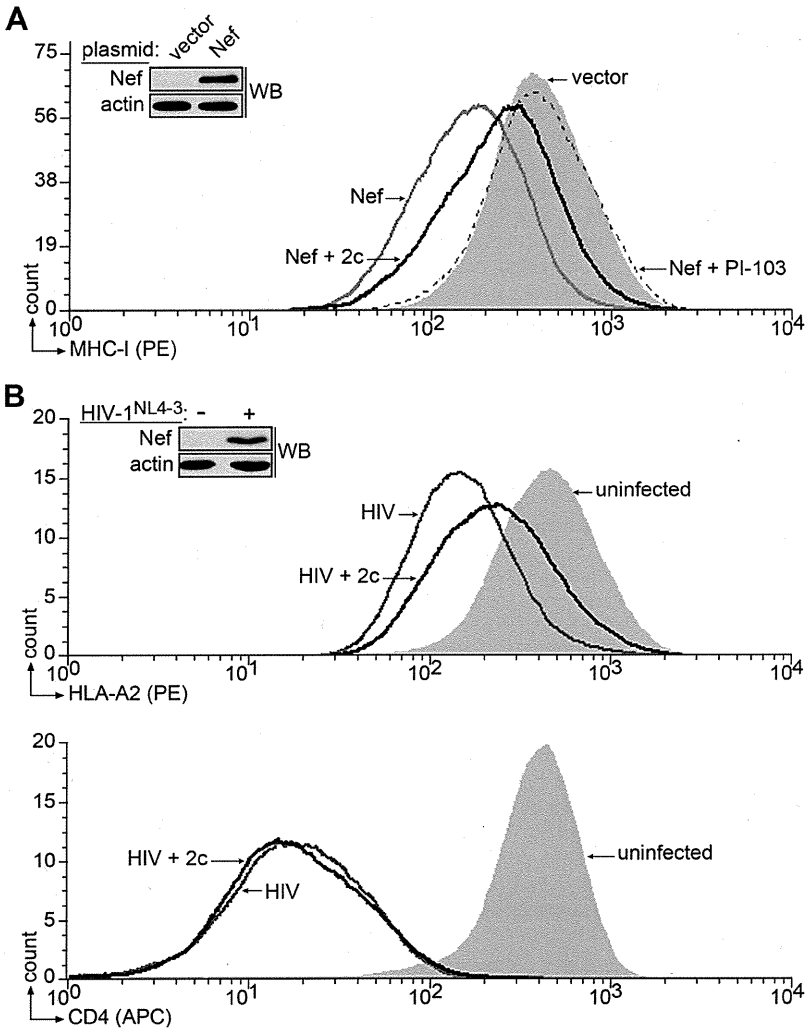

Figure 2. 2c represses HIV-1-induced down-regulation of MHC-I but not CD4. (A) H9 cells expressing eYFP (vector) or Nef-eYFP (Nef) for 24 h were treated or not with 20 μM 2c (Nef + 2c) or 5 μM of the class I PI3K inhibitor, PI-103 (Nef + PI-103) for another 16 h. At 40 h, cultures were analyzed by flow cytometry using W6/32. MFI: vector = 479, Nef = 208, Nef + 2c = 312, Nef + PI-103 = 444. Inset: Western blot showing expression of Nef-eYFP and actin. (B) Parallel cultures of primary CD4$^+$ T-cells were infected with HIV-1^{NL4-3} and treated or not with 20 μM 2c at days 5 and 7 postinfection. At 8 d postinfection the cells were stained with p24-FITC, BB7.2, and CD4-APC and then analyzed for down-regulation of HLA-A2 (top) and CD4 (bottom) by flow cytometry as described in Methods. MHC-I MFI: uninfected = 518, HIV = 193, HIV + 2c = 301. CD4 MFI: uninfected = 413, HIV = 25.1, HIV + 2c = 25.2. Inset: Western blot showing expression of Nef and actin.

ingly, we found that GST-MHC-I CD-Nef$_{LL/AA}$ captured PACS-1 but not PACS-2, consistent with our determination that Nef requires PACS-1 subsequent to PI3K stimulation to down-regulate MHC-I (Figure 4C, right). Moreover, similar to our findings with AP-1, 2c failed to disrupt the interaction of GST-MHC-I CD-Nef$_{LL/AA}$ with PACS-1. To further evaluate whether 2c disrupts MHC-I down-regulation downstream of PI3K stimulation, we repeated the antibody uptake experiment (Figure 4D). We found that 2c blocked the ability of Nef but not Nef$_{AXXA}$-PI3K* to down-regulate MHC-I, indicating 2c specifically acts upstream of PI3K stimulation.

PTEN-Null CEM Cells Fail to Phenocopy Nef Action in Primary CD4$^+$ or H9 Cells

Our results using primary CD4$^+$ T-cells and H9 cells suggest 2c disrupts HIV-1–mediated MHC-I down-regulation by interfering with the ability of Nef to assemble the SFK-ZAP-70/Syk-PI3K complex. This signaling pathway explains the importance of the EEEE$_{65}$ and PXXP$_{75}$ sites, which trigger MHC-I internalization and subsequent M$_{20}$-mediated sequestering of internalized MHC-I molecules (Blagoveshchenskaya *et al.*, 2002; Hung *et al.*, 2007). However, an alternate model of MHC-I down-regulation, which largely relies on CEM T-cells stably expressing MHC-I, envisions a PI3K-independent pathway based largely on the M$_{20}$-mediated stoichiometric block of newly synthesized MHC-I molecules en route to the cell surface (Kasper and Collins, 2003). We therefore transfected CEM cells with plasmids expressing PTEN alone or together with Nef (Figure 5A), and tested whether 2c or PI-103 would repress MHC-I down-regulation. Because transfected PTEN can be inhibited by oxidation in leukemic cells, these experiments were conducted in 0.5 mM β-mercaptoethanol (Silva *et al.*, 2008). In contrast to H9 cells or primary CD4$^+$ T-cells, both compounds failed to repress MHC-I down-regulation in CEM cells (Figure 5B, top), suggesting Nef may down-regulate MHC-I in CEM cells by a mechanism different from it uses in H9 or primary CD4$^+$ T-cells. Alternatively, the disparate findings may have resulted from the dysregulated PI3K signaling inherent to CEM cells, which would override the requirement for the multi-kinase complex (Astoul *et al.*, 2001). Indeed, many leukemic cell lines such as CEM and Jurkat lack the tumor suppressor PTEN, which is a lipid phosphatase that attenuates PI3K signaling by dephosphorylating PIP$_3$. Thus, loss of PTEN results in constitutively elevated levels of PI3K/Akt signaling characteristic of many tumor cell lines. Although acute treatment of CEM or Jurkat cells with PI3K inhibitors

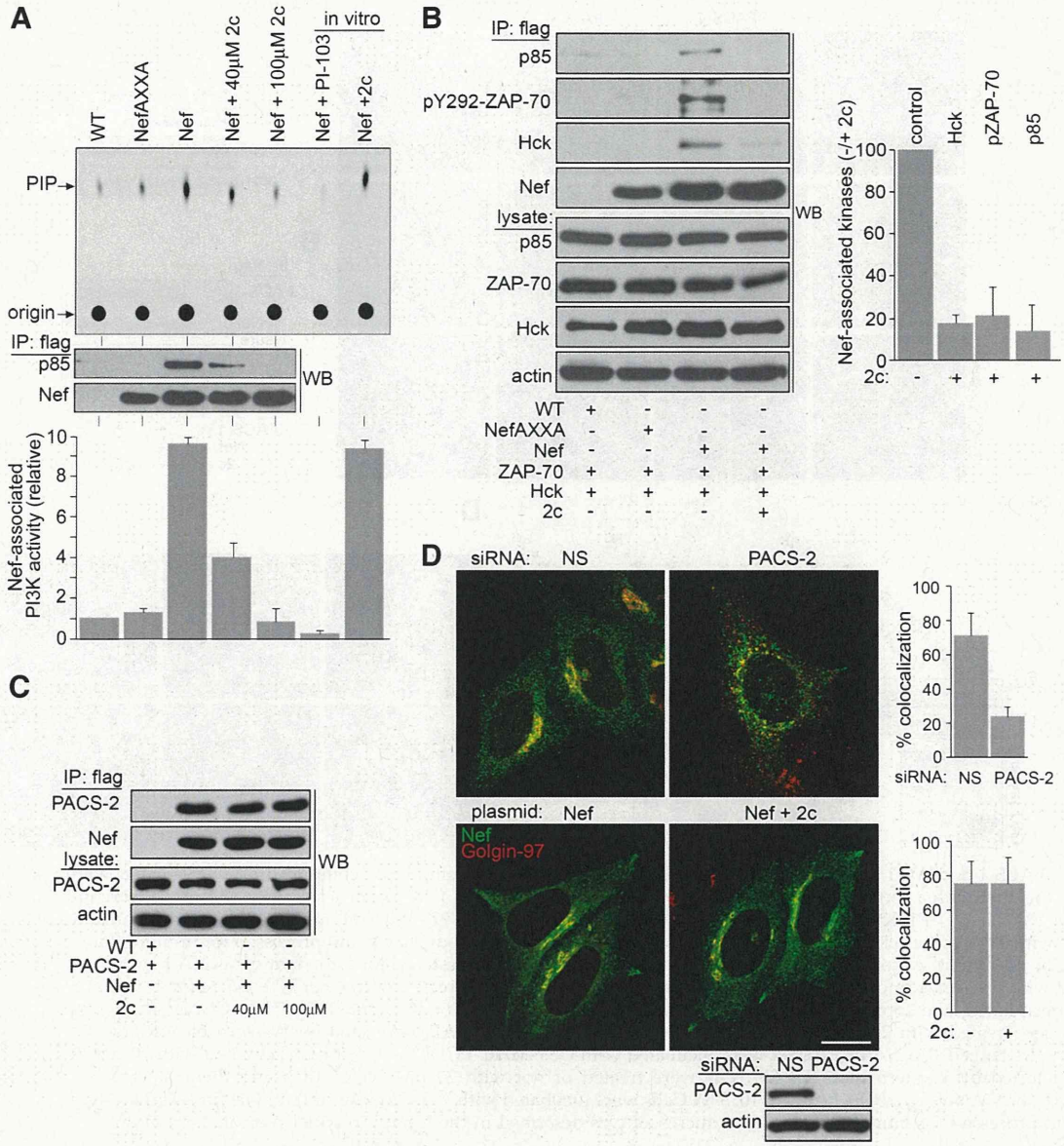

Figure 3. 2c blocks the ability of Nef to assemble the multi-kinase complex. (A) H9 cells were infected with VV:WT, VV:Nef$_{AXXA}$/f, or VV:Nef/f (moi = 10, 8 h) and treated with 40 or 100 μM 2c for 4 h (which showed no toxicity in this time frame, supplemental Figure S3, b and c). Nef/f was immunoprecipitated and Nef-associated class I PI3K p85 regulatory subunit was detected by Western blot, and associated PI3K activity was measured using an in vitro lipid kinase assay as described in Methods. As controls, 40 μM 2c and 1 μM PI-103 were incubated with the eluted fraction for 10 min before kinase assay (in vitro samples). Each assay was measured in triplicate and results are presented as the mean ± SD. (B) Left: H9 cells were coinfected with VV:WT, VV:Nef$_{AXXA}$/f, or VV:Nef/f (moi = 6, 8 h) and VV:ZAP70 (moi = 4, 8 h). Nef/f was immunoprecipitated and coprecipitating Hck, phospho-ZAP-70 and p85 were detected by Western blot. Right: The amount of each Nef-associated kinase was quantified with Image J and presented numerically as the relative amount of Nef-associated kinase ± 20 μM 2c. Error bars represent the mean ± SD from 3 independent experiments. (C) H9 cells were coinfected with VV:Nef/f (moi = 6, 8 h) and VV:PACS-2 (moi = 4, 8 h) and treated with 40 or 100 μM 2c for 4 h before harvest. Nef/f was immunoprecipitated and coprecipitating PACS-2 was detected by Western blot. (D) Upper: HeLa cells expressing Nef-eYFP together with a control siRNA (NS) or PACS-2 siRNA (Western blot of siRNA knockdown shown at bottom). Lower: HeLa cells expressing Nef-eYFP were treated with 20 μM 2c for 16 h. Cells were stained with anti-Golgin 97 (red) and visualized by confocal microscopy (scale bar, 10 μm). Morphometric analysis was performed as described in Methods. Error bars are presented as the mean ± SD from at least 20 cells per condition and three independent experiments.

prevents new PIP_3 synthesis, the absence of PTEN results in persistently elevated levels of PIP_3 that mediate PI3K-stimulated pathways even in the presence of PI3K inhibitors, thereby conferring resistance to the effect of multi-kinase complex inhibition (Hung *et al.*, 2007). We therefore expressed PTEN alone or PTEN together with Nef (Figure 5A) and determined that PTEN alone had little effect on the cell-surface levels of endogenous MHC-I, which is expected because this enzyme is normally expressed in $CD4^+$ T-cells (Figure 5B, bottom). Reexpression of PTEN, however, repressed the constitutively elevated PI3K/Akt signaling present in CEM cells as determined by a decrease in active

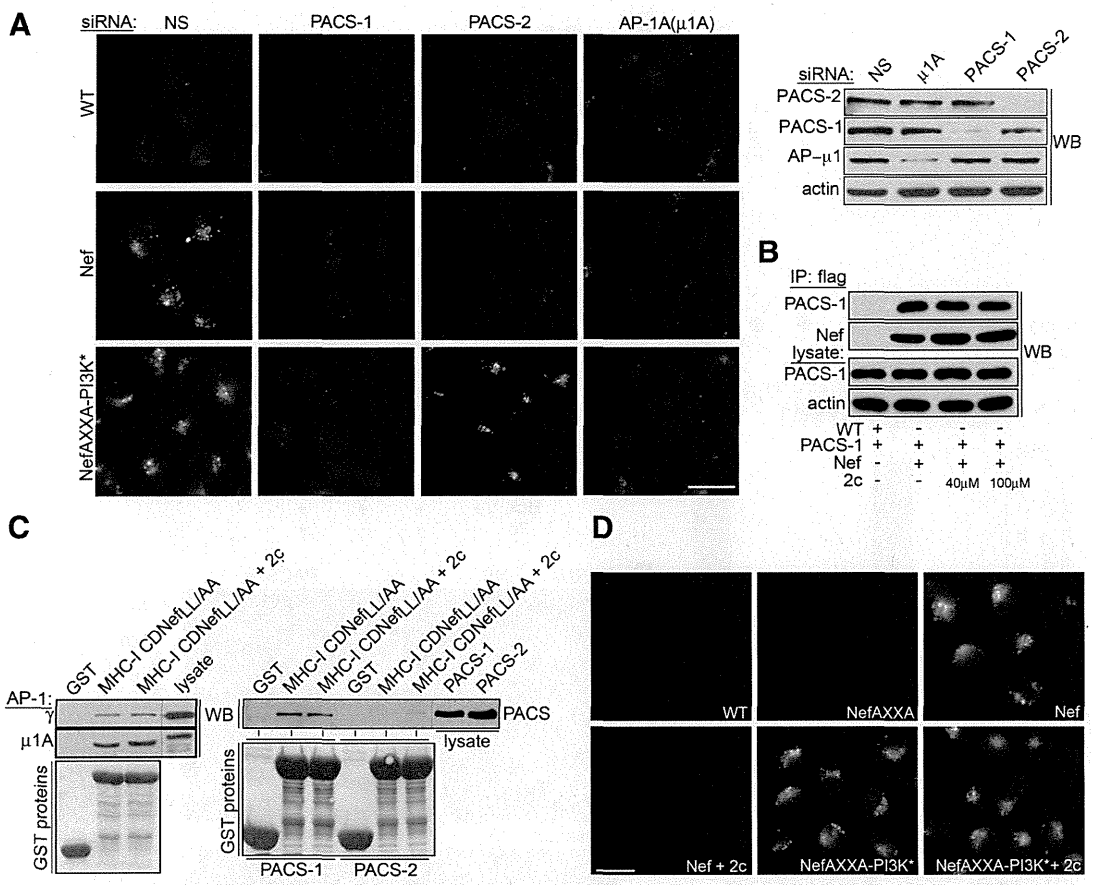

Figure 4. PACS-1 and AP-1 are required downstream of the 2c-sensitive multi-kinase complex. (A) Left: H9 cells were nucleofected with pmaxGFP together with a control siRNA (NS) or siRNAs specific for PACS-1, PACS-2, or μ1A. After 48 h, cells were infected with VV:WT, VV:Nef, or VV:Nef_{AXXA}-P13K* (moi = 10, 5 h). Cells were incubated with W6/32 (3 μg/ml) for 30 min, chased for an additional 30 min, then incubated with 0.5% acetic acid (pH 3.0) in 0.5M NaCl to remove surface antibody, fixed, and processed for immunofluorescence microscopy. Scale bar, 10 μm. Right: A portion of the cells from left were analyzed by Western blot for extent of siRNA knockdown. (B) H9 cells were coinfected with VV:Nef/f (moi = 6, 8 h) and VV:PACS-1 (moi = 4, 8 h) and treated with 40 or 100 μM 2c for 4 h before harvest. Nef/f was immunoprecipitated, and coprecipitating PACS-1 was analyzed by western blot. (C) Left: GST-MHC-I $CDNef_{LL/AA}$ or GST was mixed with A7 cell lysate, treated with 20 μM 2c, and captured g or 1μA subunits of AP-1 detected by Western blot. Right: Lysates from A7 cells expressing HA-tagged PACS-1 or PACS-2 were incubated with GST-MHC-I $CDNef_{LL/AA}$ or GST, treated with 20 μM 2c, and bound PACS proteins detected by Western blot. (D) H9 cells were treated or not with 20 μM 2c for 18 h and then infected with VV:WT, VV:Nef, VV:Nef_{AXXA}, or VV:Nef_{AXXA}-P13K* (moi = 10, 5 h). Cells were incubated with W6/32 (3 μg/ml) for 30 min and then chased for an additional 30 min and processed for immunofluorescence microscopy as described in the legend to panel A. Scale bar, 10 μm.

(phosphorylated) Akt (Figure 5A), suggesting that PTEN-replete CEM cells may be rescued in their ability to regulate PIP_3 levels and would thus be responsive to treatment with PI3K inhibitors. Accordingly, reexpression of PTEN rescued the ability of PI-103 or 2c to repress MHC-I down-regulation in CEM cells, similar to that observed in primary $CD4^+$ T-cells or H9 cells (Figure 5B bottom and see Figure 2). These results demonstrate that an intact PI3K regulatory network is required to study PI3K-dependent steps in signaling pathways, including Nef-induced MHC-I down-regulation.

Nef Down-Regulates MHC-I by a PI3K-Triggered Endocytic Pathway Followed by a Transport Block

Whereas aberrant phosphoinositide metabolism in CEM cells can explain the confusion underlying the requirement by Nef for the multi-kinase complex to down-regulate MHC-I (Kasper and Collins, 2003; Schaefer *et al.*, 2008), this defect did not readily explain why some studies found that Nef blocks delivery of newly synthesized MHC-I molecules en route to the cell surface—the stoichiometric model—whereas other studies found Nef relies on its ability to assemble the multi-kinase complex to internalize and sequester MHC-I molecules following their delivery to the cell surface—the signaling model. Although these disparate findings were originally attributed to uncharacterized differences in Golgi-to-cell-surface transport in T-cells versus HeLa cells (Kasper and Collins, 2003), closer inspection of the experimental paradigm revealed that the signaling model assessed MHC-I transport at 7–44 h postinfection while the stoichiometric model assessed ER-to-cell surface transport of MHC-I at longer postinfection times (Blagoveshchenskaya *et al.*, 2002; Kasper *et al.*, 2005; Hung *et al.*, 2007). We therefore conducted a time course to measure the ability of Nef to impede cell surface delivery of newly synthesized endogenous MHC-I molecules (Figure 6A). Parallel cultures of H9 cells infected for 24, 48, or 72 h with pseudotyped $HIV\text{-}1^{NL4\text{-}3}$ that either lack or express Nef were subjected to pulse-chase/surface biotinylation to monitor

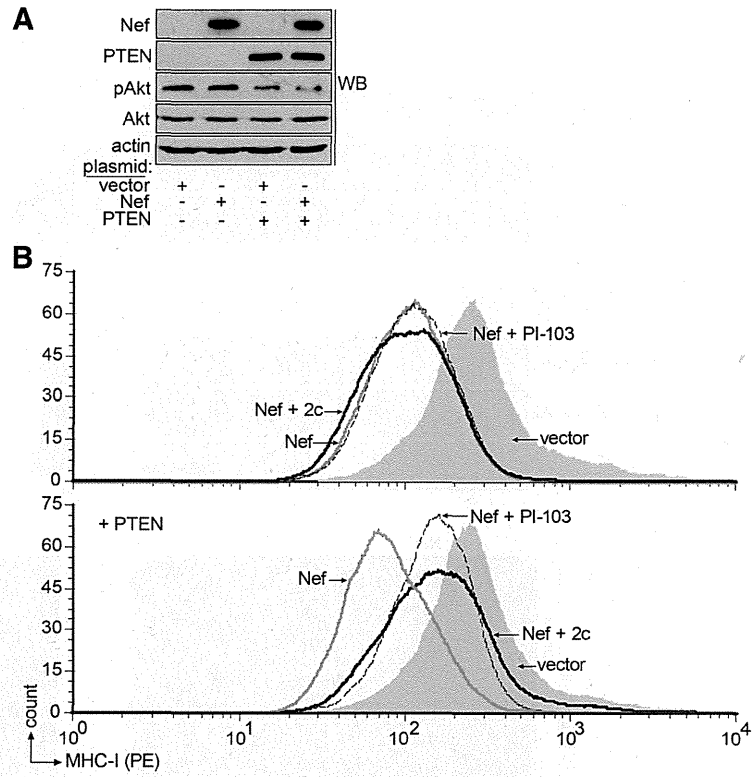

Figure 5. CEM cells do not model primary CD4$^+$ T-cells in Nef action. (A) Western blot analysis of PI3K-dysregulated CEM cells rescued or not for PTEN. (B) Top: CEM cells expressing eYFP (vector) or Nef-eYFP (Nef) were treated or not with 20 μM 2c (Nef + 2c) for 16 h before analysis or 1 μM PI-103 (Nef + PI-103) for 3 h before analysis in media containing 0.5 mM ß-mercaptoethanol. Cells were analyzed by flow cytometry using W6/32 as described in Methods. MFI: vector = 425, Nef = 125, Nef + 2c = 123, Nef + PI-103 = 128. Bottom: CEM cells expressing PTEN with either eYFP (vector) or Nef-eYFP (Nef) were processed as described above. MFI: vector = 384, Nef = 94.6, Nef + 2c = 232, Nef + PI-103 = 162.

delivery of MHC-I to the cell surface. At 24 and 48 h postinfection, Nef had no measurable effect on the transport of newly synthesized MHC-I to the cell-surface. By 72 h postinfection, however, Nef markedly repressed MHC-I transport. To test whether these results were specific to H9 cells or the use of HC10, which recognizes denatured HLA-B and C heavy chains, we repeated the pulse-chase/surface biotinylation in primary CD4$^+$ T-cells using the conformation dependent antibody, BB7.2, which recognizes HLA-A2. In agreement with our findings in H9 cells, Nef had no appreciable effect on cell-surface delivery of HLA-A2 for the first 48 h postinfection in primary CD4$^+$ T-cells. Again, similar to H9 cells, at 72 h postinfection Nef markedly repressed HLA-A2 transport to the cell surface (Figure 6B).

To determine whether the switch in Nef-induced MHC-I down-regulation was coupled with a change in MHC-I stability, H9 cells infected with Nef$^-$ or Nef$^+$ pseudotyped HIV-1 for 24 or 72 h were pulse-labeled with [^{35}S]Met/Cys for 15 min and chased for up to 20 h. Immunoprecipitation of endogenous MHC-I with HC10 showed that Nef had no obvious effect on MHC-I stability at 24 or 72 h postinfection (Figure S6). To assess whether Nef altered the rate of MHC-I transport, the immunoprecipitates were subjected to endoglycosidase H (Endo H) digestion, which demonstrated MHC-I molecules became Endo H resistant by 4 h postinfection irrespective of Nef expression or the time postinfection (Figure 6C). These findings suggest Nef does not impede MHC-I transport from early secretory pathway compartments nor does it markedly affect the stability of endogenous MHC-I molecules.

The inability of Nef to block ER-to-cell surface transport of MHC-I molecules for at least 48 h postinfection suggested that for the first two days Nef may down-regulate MHC-I by triggering the multi-kinase–dependent internalization and sequestering of MHC-I molecules from the cell surface. We tested this possibility using antibody uptake. H9 cells were infected with Nef$^+$ or Nef$^-$ pseudotyped HIV-1 for 48 or 72 h and then incubated with anti–MHC-I (W6/32) in the absence or presence of 2c or PI-103. The cells were then fixed, permeabilized, and stained with a secondary antibody to detect internalized MHC-I (W6/32) and with antibody K455 to detect steady-state MHC-I (Figure 6D). In agreement with the biotinylation analysis, at 48 h postinfection Nef induced a marked increase in MHC-I internalization that overlapped with the MHC-I post-fix staining pattern. Treatment of the cells with 2c or PI-103 blocked antibody uptake, suggesting multi-kinase complex formation was required to down-regulate MHC-I at these time points. By contrast, at 72 h postinfection Nef failed to induce W6/32 uptake despite down-regulating MHC-I as determined by the K455 post-fix staining pattern. Analysis by flow cytometry revealed that Nef reduced cell surface levels of MHC-I to a similar extent at 48 h or 72 h postinfection (Figure 6E). Together, these experiments suggest that Nef-induced MHC-I down-regulation is manifest for two days by a Nef-assembled PI3K signaling pathway that sequesters MHC-I endocytosed from the cell-surface followed by a switch in Nef action at day three to a stoichiometric mechanism that prevents ER to cell surface transport of newly synthesized MHC-I.

The Signaling Mode Is Required for the Switch to the Stoichiometric Mode

The switch in Nef-induced MHC-I down-regulation from a signaling-based pathway to a stoichiometric mechanism did not appear to result from use of tumor cell lines, differences in antibodies used to immunoprecipitate MHC-I, or levels of Nef expression (see Figure 6). We therefore asked whether

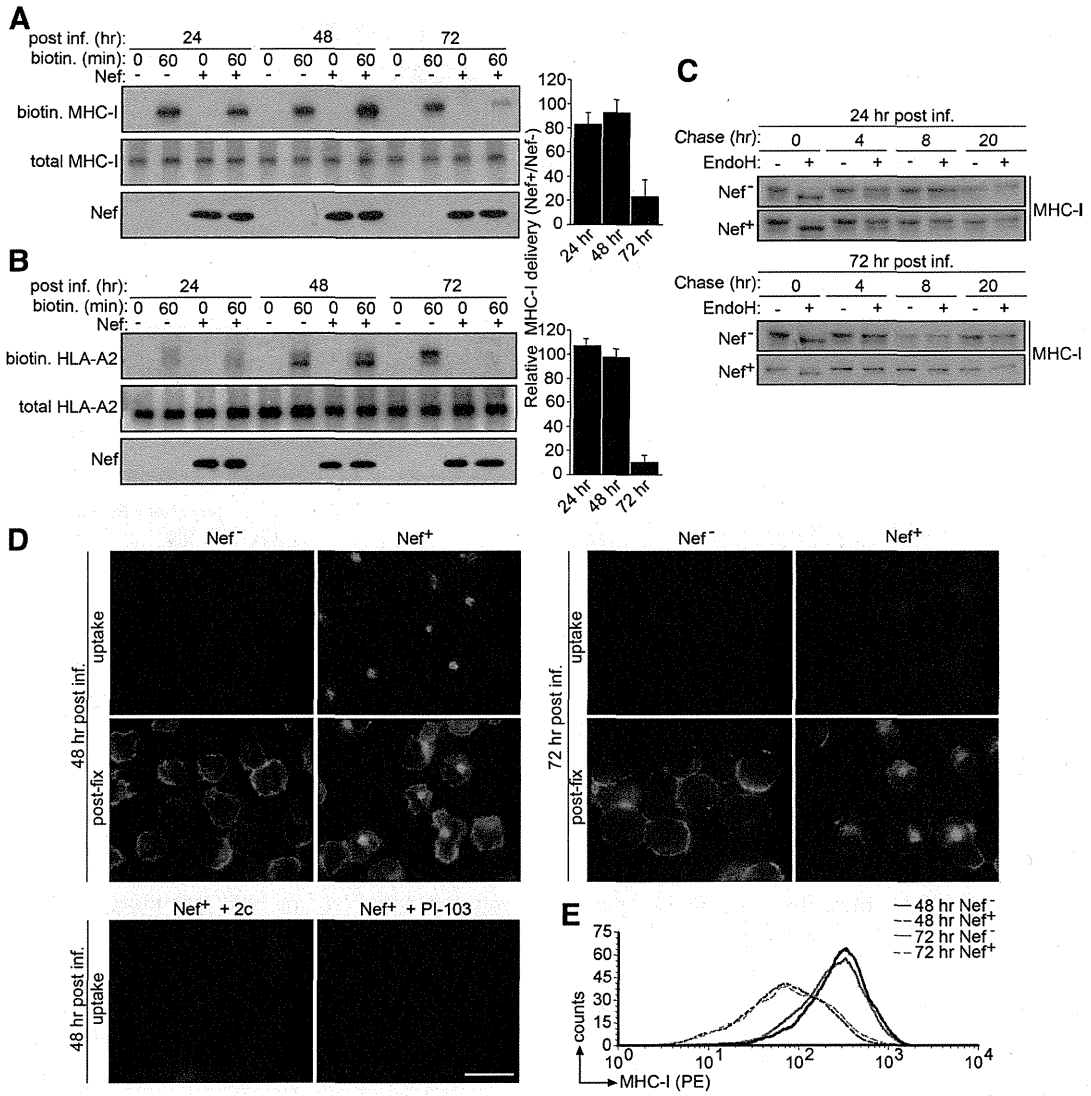

Figure 6. Nef-induced MHC-I down-regulation switches from a signaling to a stoichiometric mechanism. (A) H9 cells infected with Nef$^-$ or Nef$^+$ pseudotyped HIV-1^{NL4-3} viruses (moi = 2.3) for 24, 48, or 72 h and subjected to pulse-chase/surface biotinylation using HC10 associated MHC-I and quantified as described in Methods. Error bars represent the mean ± SD from 3 independent experiments. Cell viability was greater than 95% at each time point as measured by trypan blue exclusion and greater than 90% of the cells were infected with each virus as determined by GFP staining. (B) Primary CD4$^+$ T-cells were processed and quantified as in panel A except using BB7.2 to IP native MHC-I. (C) H9 cells were infected with Nef$^-$ or Nef$^+$ pseudotyped HIV-1^{NL4-3} viruses for 24 or 72 h, MHC-I was immunoprecipitated with mAb HC10 as in A and then digested or not with Endo H as described in Methods. (D) H9 cells were infected with Nef$^-$ or Nef$^+$ pseudotyped HIV-1^{NL4-3} viruses for 48 or 72 h and then treated or not with PI-103 (5 μM) or 2c (20 μM) for 16 h. Cells were incubated with W6/32 (3 μg/ml) for 30 min and then chased and processed for immunofluorescence microscopy as described in the legend to Figure 4A. Post-fix: Total MHC-I was detected post-fixation by staining the cells with K455. Scale bar, 10 μm. (E) H9 cells were infected with Nef$^-$ or Nef$^+$ pseudotyped HIV-1^{NL4-3} viruses for 48 or 72 h and analyzed for down-regulation of MHC-I as described in Methods. MFI: 48 h Nef$^-$ = 341, 48 h Nef$^+$ = 110, 72 h Nef$^-$ = 302, 72 h Nef$^+$ = 125.

the conversion of Nef-induced MHC-I down-regulation from a signaling- to a stoichiometric-mode depended upon the activity of the multi-kinase complex. To test this possibility, replicate plates of H9 cells were infected with Nef$^-$ or Nef$^+$ pseudotyped HIV-1 and then treated with 2c or PI-103 at 24 or 48 h postinfection. At 72 h postinfection, the level of cell-surface MHC-I was analyzed by flow cytometry, demonstrating that addition of 2c or PI-103 for 24 or 48 h repressed the ability of Nef to down-regulate MHC-I (supplemental Figure S7). Next, the cells were subjected to the pulse-chase/surface biotinylation assay. In agreement with the results in Figure 6 and the flow cytometry results, Nef expressed for 72 h repressed delivery of newly synthesized MHC-I to the cell surface (Figure 7). By contrast, treatment of the infected cells with either 2c or PI-103 for as little as 24 h before the pulse-chase/surface biotinylation prevented Nef from blocking cell-surface delivery of MHC-I (Figure 7, A and B, respectively). Together, these results suggest that sustained PI3K signaling driven by the multi-kinase complex is required for Nef-induced MHC-I down-regulation to switch from a signaling to a stoichiometric mode.

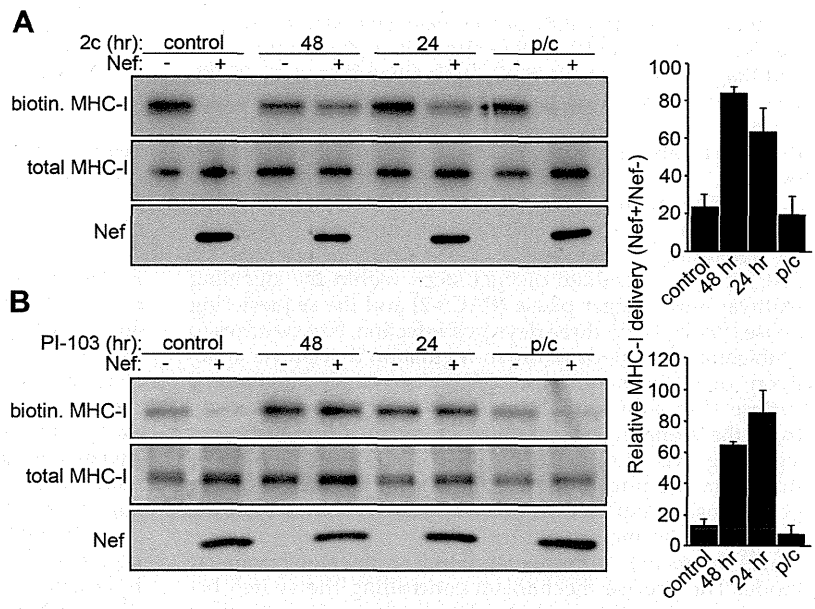

Figure 7. The PI3K signaling pathway is required for stoichiometric inhibition of MHC-I. (A) H9 cells were infected with Nef$^-$ or Nef$^+$ pseudotyped HIV-1^{NL4-3} viruses for a total of 72 h and either left untreated (control) or pretreated with 20 μM 2c for 48 h (2c 48 h) or 24 h (2c 24 h) before analysis at 72 h postinfection. The cells were then subjected to pulse-chase/surface biotinylation as described in Methods. The amount of HC10 associated MHC-I delivered to the cell surface was quantified as described in Methods. Error bars are presented as the mean ± SD from three independent experiments. (B) H9 cells were infected as above and left untreated (control) or pretreated with 5 μM PI-103 for 48 h (PI-103 48 h) or 24 h (PI-103 24 h) before analysis at 72 h postinfection and then processed as in panel A. The amount of MHC-I delivered to the cell surface was quantified as described in Methods. Error bars are presented as the mean ± SD from three independent experiments. (p/c), cells treated with 20 μM 2c (A) or 10 μM PI-103 (B) during the pulse-chase only.

DISCUSSION

We report that Nef directs a highly regulated program to down-regulate MHC-I consisting of the sequential use of the signaling and stoichiometric modes of action. During the first two days after infection, Nef uses the signaling mode to down-regulate MHC-I. This mode requires the binding of Nef to a Golgi region-localized SFK that it can directly activate to assemble a multi-kinase complex that triggers down-regulation of cell-surface MHC-I in CD4$^+$ T-cells. Using the small molecule inhibitor 2c to disrupt the Nef-SFK interaction, we repressed HIV-1 mediated down-regulation of cell-surface HLA-A2 in primary CD4$^+$ T-cells. This 2c-sensitive signaling pathway is present in primary CD4$^+$ T-cells and in H9 cells, which are replete for PTEN and are sensitive to inhibition of the multi-kinase complex. CEM cells, however, lack PTEN and thus fail to phenocopy the MHC-I down-regulation pathway used in primary CD4$^+$ T-cells. By three days postinfection, Nef switches to the stoichiometric mode that prevents delivery of newly synthesized MHC-I to the cell surface. Interference with formation of the multi-kinase complex disrupts the temporally controlled block in MHC-I transport, suggesting the Nef-directed signaling and stoichiometric modes are causally linked.

A systematic analysis of the steps underlying MHC-I down-regulation suggests 2c selectively blocks Nef action early in the down-regulation pathway at the binding of Nef to SFKs, notably Hck, Lyn, or Src (Figure 1 and supplemental Figure S3). However, the ability of 2c to directly inhibit Hck (or potentially other kinases upstream of class I PI3K), albeit at higher concentrations, may also contribute to the efficacy of 2c. Our NMR studies show that 2c affects the conformation of the N-terminal polyproline helix that binds the RT loop of SH3 domains on SFKs, especially V_{74}(Figure 1). Furthermore, the NMR data identify a potential 2c binding pocket, opposite the SH3 domain binding site, in which 2c induces significant changes of the amide resonances surrounding V_{146}, which has been previously identified as essential for Nef-Hck binding (Saksela *et al.*, 1995). Interestingly, 2c induces a change in the resonance at K_{144}, which must be ubiquitylated for Nef to down-regulate CD4 (Jin *et al.*, 2008). The lack of effect of 2c on HIV-1–induced CD4 down-regulation (Figure 2), however, suggests that ubiquitylation of Nef K_{144} is unaffected by 2c. Together, these studies suggest 2c may be a weak competitive inhibitor of Nef-SFK binding or may induce an allosteric change in Nef that indirectly represses binding to SFKs, explaining why micromolar concentrations of 2c are required to inhibit MHC-I down-regulation. In support of an allosteric mechanism, Nef alleles from long-term nonprogressors that fail to activate Hck exhibit mutations at a distance from the Hck SH3 docking site on Nef (Trible *et al.*, 2007). The ability of 2c to only partially inhibit MHC-I down-regulation in plasmid transfected cells may reflect a lower efficacy of this inhibitor compared with the class I PI3K inhibitor PI-103, which completely inhibits MHC-I down-regulation irrespective of the vector used (compare Figures 2 and S7). However, 2c can completely inhibit Nef-mediated MHC-I down-regulation in pseudovirus-infected cells, suggesting length of treatment, as well as the extent and duration of Nef expression, may influence the efficacy of this compound. The dialdehyde moiety in 2c may also be subject to chemical inactivation by reactive oxygen species characteristic of HIV-1 infection, precluding maximal efficacy of this inhibitor (Figure 2 and supplemental Figure S2 and Peterhans, 1997). Nonetheless, the findings reported here, together with the determination that 2c represses the Nef-Hck-dependent down-regulation of macrophage colony-stimulating factor (M-CSF) receptor and that diphenylfuropyriminde compounds that selectively block Nef-induced Hck activation also inhibit Nef-dependent HIV-1 replication, suggest that the future generation of potent and selective drug-like molecules that disrupt Nef-SFK binding may represent an attractive approach to the generation of novel HIV-1 therapeutics (Suzu *et al.*, 2005; Hiyoshi *et al.*, 2008; Emert-Sedlak *et al.*, 2009; Hassan *et al.*, 2009).

The signaling mode requires the PACS-2-dependent, Nef-assembled SFK-ZAP-70/Syk-PI3K multi-kinase complex to trigger increased internalization of cell-surface MHC-I molecules through an ARF6-regulated endocytic pathway (Blagoveshchenskaya *et al.*, 2002; Hung *et al.*, 2007; Atkins *et al.*, 2008; Chaudhry *et al.*, 2008). The internalized molecules

are then sequestered into paranuclear compartments by a Nef M_{20}-, AP-1–, and PACS-1–dependent process (Figure 4 and Blagoveshchenskaya *et al.*, 2002; Chaudhry *et al.*, 2008). Thus, AP-1 is required for both the signaling and stoichiometric modes of MHC-I down-regulation, but whether PACS-1 is also required in the stoichiometric mode or whether PACS-1 and AP-1 mediate common or separate sorting steps required for sequestering internalized MHC-I molecules into TGN/endosomal compartments remains to be determined. Nonetheless, these findings suggest the PACS proteins mediate distinct steps within the signaling pathway—the trigger phase (PACS-2) and the sequestering phase (PACS-1). By three days postinfection, Nef switches to a stoichiometric mode of down-regulation that prevents delivery of newly synthesized MHC-I molecules to the cell surface. The ability of 2c or PI-103 to prevent conversion from the signaling to stoichiometric mode suggests that signaling events directed by one or more of the kinases that form the multi-kinase complex may either result in post-translational modification of MHC-I, or may alter the activity of the membrane trafficking machinery that mediates the switch from the signaling to the stoichiometric mode. The precise mechanism controlling the switch between the signaling and stoichiometric modes warrants further investigation.

The relative contributions of the signaling and stoichiometric modes to Nef-induced MHC-I down-regulation have been controversial, and discrepancies may have arisen from different experimental designs, choice of cell lines, and interpretation of negative results. For example, the signaling mode was initially dismissed as a result of differences in the efficiency by which Nef is able to impede cell surface delivery of MHC-I in T-cells versus HeLa cells (Kasper and Collins, 2003; Kasper *et al.*, 2005). By contrast, we determined using parallel experiments that these differences instead result from the time postinfection at which MHC-I transport is analyzed. During early times postinfection and continuing for 48 h, Nef has no effect on the ER to cell surface transport of endogenous MHC-I molecules in HeLa, H9, and primary $CD4^+$ T-cells whereas by 72 h Nef can block MHC-I transport (Figures 6 and 7 and Blagoveshchenskaya *et al.*, 2002; Hung *et al.*, 2007). This bimodal mechanism of Nef-mediated MHC-I down-regulation does not appear to result from differences in Nef expression or in the antibodies used, suggesting the modes of Nef action may be temporally regulated. Second, the failure of PI3K inhibitors to block MHC-I down-regulation in PTEN-deficient Jurkat, CEM, or U373 cells together with the confusion regarding regulation of PTEN activity in leukemic cell lines was used to assert that Nef mediates MHC-I down-regulation by a PI3K-independent mechanism (Kasper and Collins, 2003; Larsen *et al.*, 2004; Schaefer *et al.*, 2008). However, reexpression of PTEN in CEM or U373 cells restored sensitivity of Nef-mediated MHC-I down-regulation to 2c or PI3K inhibitors, whereas siRNA knockdown of PTEN in H9 T-cells rendered Nef-mediated MHC-I down-regulation resistant to PI3K inhibitors (Figure 5 and Hung *et al.*, 2007). Therefore, the determination that the mechanism of Nef-induced MHC-I down-regulation in primary $CD4^+$ T-cells is phenocopied by H9 cells but not CEM cells underscores the importance of choice of cell lines used to model Nef action (Figure 5). Thus, the ability of PTEN-deficient CEM and U373 tumor cells to override the requirement for the SFK-ZAP-70/Syk-PI3K multi-kinase complex in triggering Nef action likely explains the confusion in the literature regarding the importance of Nef sites in MHC-I down-regulation (Kasper and Collins, 2003; Larsen *et al.*, 2004; Casartelli *et al.*, 2006; Noviello *et al.*, 2008; Schaefer *et al.*, 2008). For example, the assertion that the $AXXA_{75}$ mutation nonspecifically disrupts MHC-I down-regulation in PTEN-null cells (Swann *et al.*, 2001; Casartelli *et al.*, 2006) conflicts with the ability of Nef_{AXXA}-PI3K* to rescue MHC-I down-regulation in H9 cells (Figure 4) and with the pharamacologic repression of MHC-I down-regulation by treatment of primary $CD4^+$ T-cells with PI-103, which inhibits class I PI3K, or with 2c or D1, which block the Nef-SFK interaction (Betzi *et al.*, 2007; Hung *et al.*, 2007; Hiyoshi *et al.*, 2008; Emert-Sedlak *et al.*, 2009 and Figures 1 and 2). Reliance on PTEN-deficient cell lines may not only have caused confusion in understanding the mechanism of MHC-I down-regulation but may have also contributed to conflicting findings in HIV-1 research ranging from the signaling pathways that reactivate latent HIV-1 to the secretion of HIV-1 Tat (Bosque and Planelles, 2009; Rayne *et al.*, 2010). Third, the failure of a dominant negative dynamin mutant, which interferes with clathrin-dependent endocytosis, to block MHC-I down-regulation was used to suggest that Nef does not direct MHC-I endocytosis (Swann *et al.*, 2001). However, MHC-I is internalized by a clathrin/dynamin/AP-2-independent, ARF6-dependent pathway—both basally and in response to Nef (Le Gall *et al.*, 2000; Blagoveshchenskaya *et al.*, 2002; Caplan *et al.*, 2002; Naslavsky *et al.*, 2003; Hung *et al.*, 2007; Chaudhry *et al.*, 2008). Fourth, the ability of GST-MHC-I CD-$Nef_{LL/AA}$ to bind AP-1 μ1 subunit in vitro was used to assert that Nef does not require PACS-1 to down-regulate MHC-I in vivo (Noviello *et al.*, 2008; Singh *et al.*, 2009). However, GST-MHC-I CD-$Nef_{LL/AA}$ can also interact with PACS-1 (Figure 4), contradicting the assumption by Guatelli *et al.* that this bacterial fusion protein interacts exclusively with AP-1 (Singh *et al.*, 2009). Instead, these protein capture data are consistent with the determination in vivo that PACS-1 mediates Nef-induced MHC-I down-regulation subsequent to PI3K stimulation (Figure 4 and Atkins *et al.*, 2008; see also Youker *et al.*, 2009 for review). Lastly, whereas Nef can induce rapid degradation of overexpressed MHC-I (Kasper and Collins, 2003; Roeth *et al.*, 2004; Kasper *et al.*, 2005; Schaefer *et al.*, 2008), we observed no marked effect on the stability or ER-to-Golgi trafficking of endogenous MHC-I (Figure 6 and supplemental Figure S6 and Blagoveshchenskaya *et al.*, 2002; Hung *et al.*, 2007). Thus, the extent to which overexpressed HLA-A2.1 is physiologically relevant to the mechanism underlying Nef-induced MHC-I down-regulation remains unclear.

The determination that Nef down-regulates MHC-I by the sequential use of the signaling mode followed by the stoichiometric mode raises the possibility that HIV-1 may adapt immune evasive strategies specific to the host cell activation state or reservoir type. Because the lifespan of activated $CD4^+$ T-cells infected with HIV-1 is less than two days (Stevenson, 2003), and Nef uses the signaling mode to down-regulate MHC-I in $CD4^+$ T-cells for two days before converting to the stoichiometric mode (Figures 6 and 7), the physiological relevance of the stoichiometric pathway in activated $CD4^+$ T-cells remains uncertain. However, Nef also assembles the multi-kinase complex in cells of monocyte lineages, of which macrophages produce a low but persistent level of virus that can last the duration of the cell's natural lifespan (Hung *et al.*, 2007; Alexaki *et al.*, 2008). Future studies on the immune evasive program directed by HIV-1 Nef will require membrane trafficking experiments in relevant cell lines to determine the relative contributions of the signaling and stoichiometric modes of Nef action. The physiological significance of Nef's bimodal MHC-I down-regulation pathway in viral reservoirs can then be correlated

to disease progression. Finally, the ability of 2c and other small molecules to repress multiple actions of Nef suggests the multi-kinase complex may be an attractive approach for HIV-1 therapeutics.

ACKNOWLEDGMENTS

The authors thank K. Früh, A. Hill, and R. Papoian for helpful discussions and critically reading the manuscript, N. Morris, H. Krishnamurthy, A. Ghering, and A. Weinberg for advice, M. Delk for NMR instrumental support, and J. Guatelli, D. Johnson, J. Douglas, L. Traub, and the National Institutes of Health (NIH) AIDS Research and Reference Reagent Program for reagents. This work was supported by CIHR fellowship HFE-87760 (to J.D.D.), NRSA T32 GM71338 (to K.M.A.), Ruth L. Kirschstein NRSA AI114149 (to L.E.S.), by the Global COE program Global Education and Research Center Aiming at the control of AIDS (to M.T. and S.S.), The Pittsburgh Center for HIV Protein Interactions via NIH grant P50GM082251 (to A.M.G.), CA81398 and AI57083 (to T.E.S.), GM060170 and AI071798 (to E.B.), and GM82251 and DK37274 (to G.T.).

REFERENCES

Alexaki, A., Liu, Y., and Wigdahl, B. (2008). Cellular reservoirs of HIV-1 and their role in viral persistence. Curr. HIV Res. *6*, 388–400.

Arold, S., Franken, P., Strub, M. P., Hoh, F., Benichou, S., Benarous, R., and Dumas, C. (1997). The crystal structure of HIV-1 Nef protein bound to the Fyn kinase SH3 domain suggests a role for this complex in altered T cell receptor signaling. Structure *5*, 1361–1372.

Astoul, E., Edmunds, C., Cantrell, D. A., and Ward, S. G. (2001). PI 3-K and T-cell activation: limitations of T-leukemic cell lines as signaling models. Trends Immunol. *22*, 490–496.

Atkins, K. M., Thomas, L., Youker, R. T., Harriff, M. J., Pissani, F., You, H., and Thomas, G. (2008). HIV-1 Nef Binds PACS-2 to Assemble a Multikinase Cascade That Triggers Major Histocompatibility Complex Class I (MHC-I) Down-regulation: analysis using short interfering RNA and knock-out mice. J. Biol. Chem. *283*, 11772–11784.

Betzi, S., Restouin, A., Opi, S., Arold, S. T., Parrot, I., Guerlesquin, F., Morelli, X., and Collette, Y. (2007). Protein protein interaction inhibition (2P2I) combining high throughput and virtual screening: Application to the HIV-1 Nef protein. Proc. Natl. Acad. Sci. USA. *104*, 19256–19261.

Blagoveshchenskaya, A. D., Thomas, L., Feliciangeli, S. F., Hung, C. H., and Thomas, G. (2002). HIV-1 Nef downregulates MHC-I by a PACS-1- and PI3K-regulated ARF6 endocytic pathway. Cell *111*, 853–866.

Bodenhausen, G., and Ruben, D. J. (1980). Natural abundance nitrogen-15 NMR by enhanced heteronuclear spectroscopy. Chemical Physics Letters *69*, 185–189.

Bosque, A., and Planelles, V. (2009). Induction of HIV-1 latency and reactivation in primary memory CD4+ T cells. Blood *113*, 58–65.

Caplan, S., Naslavsky, N., Hartnell, L. M., Lodge, R., Polishchuk, R. S., Donaldson, J. G., and Bonifacino, J. S. (2002). A tubular EHD1-containing compartment involved in the recycling of major histocompatibility complex class I molecules to the plasma membrane. EMBO J. *21*, 2557–2567.

Casartelli, N., Giolo, G., Neri, F., Haller, C., Potesta, M., Rossi, P., Fackler, O. T., and Doria, M. (2006). The Pro78 residue regulates the capacity of the human immunodeficiency virus type 1 Nef protein to inhibit recycling of major histocompatibility complex class I molecules in an SH3-independent manner. J. Gen. Virol. *87*, 2291–2296.

Chaudhry, A., Das, S. R., Jameel, S., George, A., Bal, V., Mayor, S., and Rath, S. (2008). HIV-1 Nef induces a Rab11-dependent routing of endocytosed immune costimulatory proteins CD80 and CD86 to the Golgi. Traffic *9*, 1925–1935.

Choi, H. J., and Smithgall, T. E. (2004). Conserved residues in the HIV-1 Nef hydrophobic pocket are essential for recruitment and activation of the Hck tyrosine kinase. J. Mol. Biol. *343*, 1255–1268.

Douek, D. C., Picker, L. J., and Koup, R. A. (2003). T cell dynamics in HIV-1 infection. Annu. Rev. Immunol. *21*, 265–304.

Emert-Sedlak, L., Kodama, T., Lerner, E. C., Dai, W., Foster, C., Day, B., Lazo, J. S., and Smithgall, T. E. (2009). Chemical library screens targeting an HIV-1 accessory factor/host cell kinase complex identify novel anti-retroviral compounds. ACS Chem. Biol. *20*, 939–947.

Fackler, O. T., and Baur, A. S. (2002). Live and let die: Nef functions beyond HIV replication. Immunity *16*, 493–497.

Gandhi, R. T., and Walker, B. D. (2002). Immunologic control of HIV-1. Annu. Rev. Med. *53*, 149–172.

Grzesiek, S., Bax, A., Hu, J. S., Kaufman, J., Palmer, I., Stahl, S. J., Tjandra, N., and Wingfield, P. T. (1997). Refined solution structure and backbone dynamics of HIV-1 Nef. Protein Sci. *6*, 1248–1263.

Hanna, Z., Kay, D. G., Cool, M., Jothy, S., Rebai, N., and Jolicoeur, P. (1998). Transgenic mice expressing human immunodeficiency virus type 1 in immune cells develop a severe AIDS-like disease. J. Virol. *72*, 121–132.

Hansen, T. H., and Bouvier, M. (2009). MHC class I antigen presentation: learning from viral evasion strategies. Nat. Rev. Immunol. *9*, 503–513.

Hassan, R., Suzu, S., Hiyoshi, M., Takahashi-Makise, N., Ueno, T., Agatsuma, T., Akari, H., Komano, J., Takebe, Y., Motoyoshi, K., and Okada, S. (2009). Dys-regulated activation of a Src tyroine kinase Hck at the Golgi disturbs N-glycosylation of a cytokine receptor Fms. J. Cell. Physiol. *221*, 458–468.

Hiyoshi, M., Suzu, S., Yoshidomi, Y., Hassan, R., Harada, H., Sakashita, N., Akari, H., Motoyoshi, K., and Okada, S. (2008). Interaction between Hck and HIV-1 Nef negatively regulates cell surface expression of M-CSF receptor. Blood *111*, 243–250.

Hung, C. H., Thomas, L., Ruby, C. E., Atkins, K. M., Morris, N. P., Knight, Z. A., Scholz, I., Barklis, E., Weinberg, A. D., Shokat, K. M., and Thomas, G. (2007). HIV-1 Nef assembles a Src family kinase-ZAP-70/Syk-PI3K cascade to downregulate cell-surface MHC-I. Cell Host Microbe *1*, 121–133.

Jin, Y. J., Cai, C. Y., Zhang, X., and Burakoff, S. J. (2008). Lysine 144, a ubiquitin attachment site in HIV-1 Nef, is required for Nef-mediated CD4 down-regulation. J. Immunol. *180*, 7878–7886.

Kasper, M. R., and Collins, K. L. (2003). Nef-mediated disruption of HLA-A2 transport to the cell surface in T cells. J. Virol. *77*, 3041–3049.

Kasper, M. R., Roeth, J. F., Williams, M., Filzen, T. M., Fleis, R. I., and Collins, K. L. (2005). HIV-1 Nef disrupts antigen presentation early in the secretory pathway. J. Biol. Chem. *280*, 12840–12848.

Larsen, J. E., Massol, R. H., Nieland, T. J., and Kirchhausen, T. (2004). HIV Nef-mediated major histocompatibility complex class I down-modulation is independent of Arf6 activity. Mol. Biol. Cell *15*, 323–331.

Le Gall, S., Buseyne, F., Trocha, A., Walker, B. D., Heard, J. M., and Schwartz, O. (2000). Distinct trafficking pathways mediate Nef-induced and clathrin-dependent major histocompatibility complex class I down-regulation. J. Virol. *74*, 9256–9266.

Lee, C. H., Leung, B., Lemmon, M. A., Zheng, J., Cowburn, D., Kuriyan, J., and Saksela, K. (1995). A single amino acid in the SH3 domain of Hck determines its high affinity and specificity in binding to HIV-1 Nef protein. EMBO J. *14*, 5006–5015.

Lieberman, J. (2003). The ABCs of granule-mediated cytotoxicity: new weapons in the arsenal. Nat. Rev. Immunol. *3*, 361–370.

Matsuda, D., Nakayama, Y., Horimoto, S., Kuga, T., Ikeda, K., Kasahara, K., and Yamaguchi, N. (2006). Involvement of Golgi-associated Lyn tyrosine kinase in the translocation of annexin II to the endoplasmic reticulum under oxidative stress. Exp. Cell Res. *312*, 1205–1217.

Naslavsky, N., Weigert, R., and Donaldson, J. G. (2003). Convergence of non-clathrin- and clathrin-derived endosomes involves Arf6 inactivation and changes in phosphoinositides. Mol. Biol. Cell *14*, 417–431.

Noviello, C. M., Benichou, S., and Guatelli, J. C. (2008). Cooperative binding of the class I major histocompatibility complex cytoplasmic domain and human immunodeficiency virus type 1 Nef to the endosomal AP-1 complex via its mu subunit. J. Virol. *82*, 1249–1258.

Oneyama, C., Agatsuma, T., Kanda, Y., Nakano, H., Sharma, S. V., Nakano, S., Narazaki, F., and Tatsuta, K. (2003). Synthetic inhibitors of proline-rich ligand-mediated protein-protein interaction: potent analogs of UCS15A. Chem. Biol. *10*, 443–451.

Peterhans, E. (1997). Oxidants and antioxidants in viral diseases: disease mechanisms and metabolic regulation. J. Nutr. *127*, 962S–965S.

Peterlin, B. M., and Trono, D. (2003). Hide, shield and strike back: how HIV-infected cells avoid immune eradication. Nat. Rev. Immunol. *3*, 97–107.

Piguet, V., Wan, L., Borel, C., Mangasarian, A., Demaurex, N., Thomas, G., and Trono, D. (2000). HIV-1 Nef protein binds to the cellular protein PACS-1 to downregulate class I major histocompatibility complexes. Nat. Cell Biol. *2*, 163–167.

Pulvirenti, T., Giannotta, M., Capestrano, M., Capitani, M., Pisanu, A., Polishchuk, R. S., San Pietro, E., Beznoussenko, G. V., Mironov, A. A., Turacchio, G., Hsu, V. W., Sallese, M., and Luini, A. (2008). A traffic-activated Golgi-based signalling circuit coordinates the secretory pathway. Nat. Cell Biol. *10*, 912–922.

Rayne, F., Debaisieux, S., Yezid, H., Lin, Y. L., Mettling, C., Konate, K., Chazal, N., Arold, S. T., Pugniere, M., Sanchez, F., Bonhoure, A., Briant, L., Loret, E., Roy, C.,

and Beaumelle, B. (2010). Phosphatidylinositol-(4,5)-bisphosphate enables efficient secretion of HIV-1 Tat by infected T-cells. EMBO J. *29*, 1348–1362.

Roeth, J. F., Williams, M., Kasper, M. R., Filzen, T. M., and Collins, K. L. (2004). HIV-1 Nef disrupts MHC-I trafficking by recruiting AP-1 to the MHC-I cytoplasmic tail. J. Cell Biol. *167*, 903–913.

Saksela, K., Cheng, G., and Baltimore, D. (1995). Proline-rich (PxxP) motifs in HIV-1 Nef bind to SH3 domains of a subset of Src kinases and are required for the enhanced growth of Nef+ viruses but not for down-regulation of CD4. EMBO J. *14*, 484–491.

Schaefer, M. R., Wonderlich, E. R., Roeth, J. F., Leonard, J. A., and Collins, K. L. (2008). HIV-1 Nef targets MHC-I and CD4 for degradation via a final common beta-COP-dependent pathway in T cells. PLoS Pathog. *4*, e1000131.

Silva, A., Yunes, J. A., Cardoso, B. A., Martins, L. R., Jotta, P. Y., Abecasis, M., Nowill, A. E., Leslie, N. R., Cardoso, A. A., and Barata, J. T. (2008). PTEN posttranslational inactivation and hyperactivation of the PI3K/Akt pathway sustain primary T cell leukemia viability. J. Clin. Invest. *118*, 3762–3774.

Simmen, T., Aslan, J. E., Blagoveshchenskaya, A. D., Thomas, L., Wan, L., Xiang, Y., Feliciangeli, S. F., Hung, C. H., Crump, C. M., and Thomas, G. (2005). PACS-2 controls endoplasmic reticulum-mitochondria communication and Bid-mediated apoptosis. EMBO J. *24*, 717–729.

Singh, R. K., Lau, D., Noviello, C. M., Ghosh, P., and Guatelli, J. C. (2009). An MHC-I cytoplasmic domain/HIV-1 Nef fusion protein binds directly to the mu subunit of the AP-1 endosomal coat complex. PLoS One *4*, e8364.

Stevenson, M. (2003). HIV-1 pathogenesis. Nat. Med. *9*, 853–860.

Suzu, S., Harada, H., Matsumoto, T., and Okada, S. (2005). HIV-1 Nef interferes with M-CSF receptor signaling through Hck activation and inhibits M-CSF bioactivities. Blood *105*, 3230–3237.

Swann, S. A., Williams, M., Story, C. M., Bobbitt, K. R., Fleis, R., and Collins, K. L. (2001). HIV-1 Nef blocks transport of MHC class I molecules to the cell surface via a PI 3-kinase-dependent pathway. Virology *282*, 267–277.

Tomiyama, H., Akari, H., Adachi, A., and Takiguchi, M. (2002). Different effects of Nef-mediated HLA class I down-regulation on human immunodeficiency virus type 1-specific CD8(+) T-cell cytolytic activity and cytokine production. J. Virol. *76*, 7535–7543.

Trible, R. P., Emert-Sedlak, L., and Smithgall, T. E. (2006). HIV-1 Nef selectively activates Src family kinases Hck, Lyn, and c-Src through direct SH3 domain interaction. J. Biol. Chem. *281*, 27029–27038.

Trible, R. P., Emert-Sedlak, L., Wales, T. E., Ayyavoo, V., Engen, J. R., and Smithgall, T. E. (2007). Allosteric loss-of-function mutations in HIV-1 Nef from a long-term non-progressor. J. Mol. Biol. *374*, 121–129.

Yang, O. O., Nguyen, P. T., Kalams, S. A., Dorfman, T., Gottlinger, H. G., Stewart, S., Chen, I. S., Threlkeld, S., and Walker, B. D. (2002). Nef-mediated resistance of human immunodeficiency virus type 1 to antiviral cytotoxic T lymphocytes. J. Virol. *76*, 1626–1631.

Yewdell, J. W., and Hill, A. B. (2002). Viral interference with antigen presentation. Nat. Immunol. *3*, 1019–1025.

Youker, R. T., Shinde, U., Day, R., and Thomas, G. (2009). At the crossroads of homoeostasis and disease: roles of the PACS proteins in membrane traffic and apoptosis. Biochem. J. *421*, 1–15.